AIMS Mathematics

http://www.aimspress.com/journal/Math

AIMS Mathematics, 8(9): 21406–21438.
DOI: 10.3934/math.20231091
Received: 24 May 2023
Revised: 19 June 2023
Accepted: 28 June 2023
Published: 05 July 2023

Research article

A stabilized multiple time step method for coupled Stokes-Darcy flows and transport model

Jingyuan Zhang*, **Ruikun Zhang and Xue Lin**

School of Mathematics and Physics, Qingdao University of Science and Technology, Qingdao, Shandong, 266061, China

* **Correspondence:** Email: iamzjy00@126.com; Tel: +8617669609598.

Abstract: A stabilized finite element algorithm with different time steps on different physical variables for the coupled Stokes-Darcy flows system with the solution transport is studied. The viscosity in the model is assumed to depend on the concentration. The nonconforming piecewise linear Crouzeix-Raviart element and piecewise constant are used to approximate velocity and pressure in the coupled Stokes-Darcy flows system, and conforming piecewise linear finite element is used to approximate concentration in the transport system. The time derivatives are discretized with different step sizes for the partial differential equations in these two systems. The existence and uniqueness of the approximate solution are unconditionally satisfied. A priori error estimates are established, which also provides a guidance on the ratio of time step sizes with respect to the ratio of the physical parameters. Numerical examples are presented to verify the theoretical results.

Keywords: coupled Stokes and Darcy flows; soulte transport; Crouzeix-Raviart finite element; multiple time step method; error estimates
Mathematics Subject Classification: 65M12, 65M15, 65M60

1. Introduction

The models for the coupling of fluid flows in a porous medium domain and a free flow domain have a wide applications in environment science [15] and biofluid dynamics [18]. The fluid flow in the porous medium domain is described by Darcy equation, and the fluid flow in the free flow domain is modeled by Stokes equation. The two equations are coupled through the interface conditions, which connects the porous domain and the free flow domain.

For past years, stable and convergent numerical methods for the coupled Stokes and Darcy flows system can be found in many references, which have been deeply studied. For example, the coupled finite element methods [7, 23, 28], the domain decomposition methods [2, 6, 9, 37], the conforming finite volume element method [25], the non-conforming finite element methods [32, 41], the mortar finite element methods [1, 12, 21], the Lagrange multiplier methods [5, 19, 24], the mixed finite element method combining with the DG method [30, 31], the DG method combining with mimetic finite difference method [26], the staggered DG method [42], the pseudospectral least squares method [22], the spectral method [39], the weak Galerkin methods [11], and many other numerical methods [10, 17, 27, 29, 36].

The aim of this paper is to construct an efficient numerical algorithm for the Stokes-Darcy flows system coupled with the transport of a chemical. This kind of model can describe solute transport in the coupled flow region and porous media flow region, which appear in the research of human health and the environment. For example, the groundwater contamination, the pollution of groundwater by transport of contaminants through rivers. Cesmelioglu and Riviére study the existence and stability bounds of the weak solution with the fluid viscosity depending on the concentration for this model in [8]. For numerical methods, Vassilev and Yotov solve the flow equations through the domain decomposition method, and solve the transport equation by using local discontinuous Galerkin method [38]. The viscosity of the fluid in this study is assumed to be independent of the concentration. In [33], the authors study the numerical methods for the model with concentration-dependent viscosity, they propose a mixed weak formulation for the coupled flow problem, and use conforming piecewise linear finite element to approximate concentration.

In this paper, as an extended research of [33], we study the numerical methods for the Stokes-Darcy-Transport system with different time steps on coupled Stokes-Darcy flows system and the transport system. The viscosity in this study is assumed to depend on concentration. Since the Stokes-Darcy-Transport system is a multi-physics problem, the partial differential equations have different time scale reflected by the corresponding physical parameters, so it reminds us that we can use larger time step in the region with slower velocity. By using the multiple time step discrete finite element scheme, we can obtain the same optimal error estimation order as [33], and reduce computation, effectively improve computational efficiency. The multiple time step technique for the Stokes-Darcy was studied in [34,35]. In this study, we construct a stabilized mixed finite element method for the coupled Stokes-Darcy flows system by using the nonconforming piecewise linear Crouzeix-Raviart element for velocity and using piecewise constant function for pressure, and propose classical piecewise linear finite element method for the transport system. Under no assumption on the restriction about the time-step and spatial meshsize, we obtain the existence and uniqueness of the numerical solutions, and a prior error estimates. From the error analysis, we also derive the ratio of different time step sizes which should be proportional to the ratio of the physical parameters.

The rest of the article is organized as follows. In Section 2, we introduce the model problem and present the mixed weak formulation. In Section 3, we propose the multiple time step scheme with different time steps on Stokes-Darcy flows system and solute transport, and give the existence and uniqueness of the scheme by adding a stabilization term, which derive the discrete inf-sup condition. The error estimates for fluid velocity and concentration, and the relationship formula between physical parameters and the ratio of different time steps are presented in Section 4. In Section 5, we present some numerical examples to verify that the numerical results are in agreement with the theoretical analysis.

Throughout this paper we use C, with or without subscription, to denote a generic constant, which should have different values in different appearances.

2. Model problem and weak formulation

Consider the model of a flow in a bounded domain $\Omega \subset R^L(L{=}2 \text{ or } 3)$, consisting of a free region Ω_s, where the flow is governed by the Stokes equations, and a porous medium domain $\Omega_d = \Omega\backslash\overline{\Omega}_s$, where the flow is governed by Darcy's law. The two regions are separated by a interface $\Gamma_I = \partial\Omega_s \cap \partial\Omega_d$. Let $\Gamma_l = \partial\Omega_l\backslash\Gamma_I(l = s, d)$. Each interface and boundary is assumed to be polygonal. We denote by $\boldsymbol{n}_l(l = s, d)$ the unit outward normal direction on $\partial\Omega_l(l = s, d)$, and on the interface $\boldsymbol{n}_s = -\boldsymbol{n}_d$.

Figure 1 gives a schematic representation of the geometry with $L = 2$.

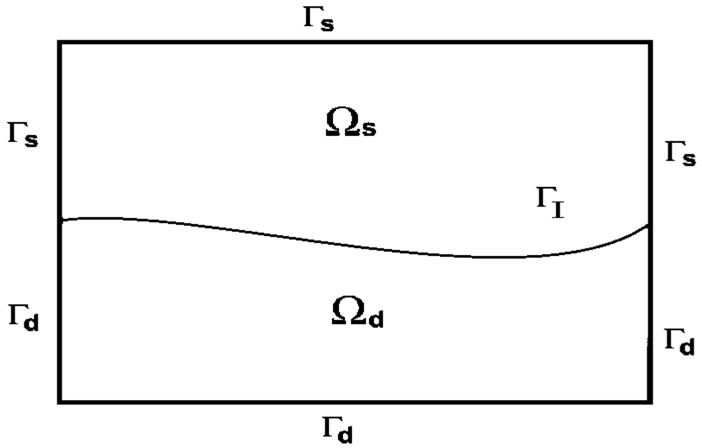

Figure 1. The model problem.

In all of Ω, denote the fluid velocity by $\boldsymbol{u}(\boldsymbol{x}, t)$, the pressure by $p(\boldsymbol{x}, t)$ and the concentration by $c(\boldsymbol{x}, t)$. For any vector and scalar functions $\boldsymbol{v}$, q defined in Ω, it often plays different mathematical roles in Ω_s and Ω_d, we will often need to distinguish them, especially their traces on Γ_I, thus define

$$\boldsymbol{v}_s = \boldsymbol{v}|_{\Omega_s}, \qquad \boldsymbol{v}_d = \boldsymbol{v}|_{\Omega_d}, \qquad q_s = q|_{\Omega_s}, \qquad and \quad q_d = q|_{\Omega_d}.$$

Let $J = [0, T_1]$ be the time interval, and ∂_t denotes the usual partial derivative $\partial/\partial t$, then in the free region Ω_s, the equations of motion, continuity and mass transport can be written as

$$\partial_t\boldsymbol{u} - \nabla\cdot(2\mu(c)\boldsymbol{S}(\boldsymbol{u})) + \nabla p = \boldsymbol{f}(c), \quad \boldsymbol{x} \in \Omega_s, t \in J, \tag{2.1}$$

$$\nabla\cdot\boldsymbol{u} = 0, \quad \boldsymbol{x} \in \Omega_s, t \in J, \tag{2.2}$$

$$\partial_t c - \nabla\cdot(d\nabla c) + \boldsymbol{u}\cdot\nabla c = 0, \quad \boldsymbol{x} \in \Omega_s, t \in J. \tag{2.3}$$

In the porous medium Ω_d, the equations of motion, continuity and mass transport can be written as

$$\lambda^{-1}(c)\boldsymbol{u} = -\nabla p, \quad \boldsymbol{x} \in \Omega_d, t \in J, \tag{2.4}$$

$$\nabla\cdot\boldsymbol{u} = q^I - q^P, \quad \boldsymbol{x} \in \Omega_d, t \in J, \tag{2.5}$$

$$\phi\partial_t c - \nabla\cdot(\boldsymbol{D}(\boldsymbol{u})\nabla c) + \boldsymbol{u}\cdot\nabla c = (c^I - c)q^I, \quad \boldsymbol{x} \in \Omega_d, t \in J. \tag{2.6}$$

where $\mu(c)$ is the concentration-dependent fluid viscosity, we will assume it by the quarter-power rule, see Eq (2.20). $\boldsymbol{S}$ is the deformation rate tensor and defined by $\boldsymbol{S}(\boldsymbol{v}) = \frac{1}{2}(\nabla\boldsymbol{v} + \nabla\boldsymbol{v}^T)$, $\boldsymbol{f} \in (L^2(\Omega))^L(L = 2 \; or \; 3)$ is a term related to body forces, d is the molecular diffusion coefficient, $\boldsymbol{D}$ is the diffusion-dispersion coefficient, $\lambda(c) = \dfrac{K(\boldsymbol{x})}{\mu(c)}$, $K = \operatorname{diag} k_j \in L^\infty(\Omega_d)^{L\times L}$ is the permeability of the medium, q^I represents a source term, q^P represents a sink term, $\phi \in L^\infty(\Omega_d)$ is the porosity of the medium, and c^I is the injected concentration.

On the interface Γ_I, the conditions are imposed

$$\begin{aligned} \boldsymbol{u}_s \cdot \boldsymbol{n}_s + \boldsymbol{u}_d \cdot \boldsymbol{n}_d &= 0, && (2.7)\\ p_s - \boldsymbol{n}_s \cdot 2\mu(c_s)\boldsymbol{S}(\boldsymbol{u}_s)\cdot \boldsymbol{n}_s &= p_d, && (2.8)\\ 2\boldsymbol{n}_s \cdot \boldsymbol{S}(\boldsymbol{u}_s)\cdot \boldsymbol{\tau}_j + \gamma_j \boldsymbol{u}_s \cdot \boldsymbol{\tau}_j &= 0,\ j = 1, \cdots, L-1, && (2.9)\\ c_s &= c_d, && (2.10)\\ d\nabla c_s \cdot \boldsymbol{n}_s + \boldsymbol{D}(\boldsymbol{u}_d)\nabla c_d \cdot \boldsymbol{n}_d &= 0. && (2.11) \end{aligned}$$

Here $\gamma_j = \alpha_1/\sqrt{k_j}$, α_1 is a parameter determined by experimental evidence. Equations (2.7), (2.10) and (2.11) represent continuity of mass flux and concentration, Eq (2.8) represents the balance of normal forces, Eq (2.9) is the Beavers-Joseph-Saffman condition. Moreover, τ_j denote a orthonormal system of tangent vectors on Γ_I.

To complete the system, we give the following boundary conditions

$$\begin{aligned} \boldsymbol{u}_s &= 0, \quad \boldsymbol{x} \in \Gamma_s, t \in J, && (2.12)\\ \boldsymbol{u}_d \cdot \boldsymbol{n}_d &= 0, \quad \boldsymbol{x} \in \Gamma_d, t \in J, && (2.13)\\ \overline{\boldsymbol{D}}(\boldsymbol{u})\nabla c \cdot \boldsymbol{n} &= 0, \quad \boldsymbol{x} \in \partial\Omega, t \in J, && (2.14) \end{aligned}$$

and initial conditions

$$\begin{aligned} \boldsymbol{u}_s(\boldsymbol{x}, 0) &= \boldsymbol{u}_{s,0}(\boldsymbol{x}), \quad \boldsymbol{x} \in \Omega_s, && (2.15)\\ c(\boldsymbol{x}, 0) &= c_0(\boldsymbol{x}), \quad \boldsymbol{x} \in \Omega. && (2.16) \end{aligned}$$

Here

$$\overline{\boldsymbol{D}} = \begin{cases} d\boldsymbol{I}, & \boldsymbol{x} \in \Omega_s, \\ \boldsymbol{D}(\boldsymbol{u}), & \boldsymbol{x} \in \Omega_d, \end{cases} \qquad (2.17)$$

where $\boldsymbol{I}$ is the identity matrix.

Equations (2.1)–(2.16) consist of the coupled Stokes and Darcy flows system with an advection-diffusion equation that models transport of a chemical in which the viscosity is dependent on the concentration c.

To facilitate the subsequent discussion, we now make the following assumptions about some physical quantities in the system.

(1) The porosity of the medium $\phi(\boldsymbol{x})$ and the permeability of the medium $K(\boldsymbol{x})$ are uniformly bounded and positive defined in Ω_d. There exists positive constants $\phi_{\max}$, $\phi_{\min}$, $k_{\max}$ and $k_{\min}$ such that

$$\phi_{\min} \le \phi(\boldsymbol{x}) \le \phi_{\max}, \quad \forall \boldsymbol{x} \in \Omega_d, \qquad (2.18)$$

$$k_{\min}|\boldsymbol{x}|^2 \le K\boldsymbol{x}\cdot\boldsymbol{x} \le k_{\max}|\boldsymbol{x}|^2,\ \forall \boldsymbol{x} \in \Omega_d. \qquad (2.19)$$

(2) The form of μ is assumed by the quarter-power rule

$$\mu(c) = \mu(0)\left[\Big(\frac{\mu(0)}{\mu(1)}\Big)^{\frac{1}{4}} c + (1-c)\right]^{-4}, \quad c \in [0,1]. \qquad (2.20)$$

From (2.20), we know that $\mu(c)$ is bounded and monotone for concentration $c \in [0, 1]$

$$\mu_{\min} \le \mu(c) \le \mu_{\max}, \quad \forall c \in [0, 1], \tag{2.21}$$

where $\mu_{\min} = \min\{\mu(1), \mu(0)\}$, $\mu_{\max} = \max\{\mu(1), \mu(0)\}$.

What's more, $\mu(c)$ is a Lipschitz continuous function for concentration $c \in [0, 1]$ with Lipschitz constant μ_L.

Thus, from the assumptions (1) and (2), λ is also bounded, monotone and Lipschitz continuous for concentration $c \in [0, 1]$, we can get the estimate inequality of λ directly

$$\frac{k_{\min}}{\mu_{\max}}|\boldsymbol{x}|^2 \le \lambda(c)\boldsymbol{x} \cdot \boldsymbol{x} \le \frac{k_{\max}}{\mu_{\min}}|\boldsymbol{x}|^2, \quad \forall c \in [0, 1], \boldsymbol{x} \in \Omega_d. \tag{2.22}$$

(3) The source term and sink term $q^I, q^P \ge 0$ satisfy the compatibility condition

$$\int_{\Omega_d} (q^I - q^P)dx = 0,$$

and $q^I, q^P \in L^\infty(J; L^2(\Omega_d))$. c^I satisfies $0 \le c^I \le 1$ *a.e. in* Ω_d^T.
(4) $\boldsymbol{f}(c)$ is a Lipschitz continuous function for concentration $c \in [0, 1]$ with Lipschitz constant f_L.
(5) The diffusion-dispersion coefficient $\boldsymbol{D}$ (refer to [16]) is taken to be

$$\boldsymbol{D}(\boldsymbol{u}) = \phi d\widetilde{\tau}\boldsymbol{I} + |\boldsymbol{u}|(d_l\boldsymbol{E}(\boldsymbol{u}) + d_t\boldsymbol{E}^\perp), \tag{2.23}$$

where $\widetilde{\tau}$ is a positive constant in $(0, 1)$, and represents the tortuosity of the porous medium, d_l and d_t are the longitudinal and transverse dispersion coefficients, respectively. For $\boldsymbol{u} = (u_1, \cdots, u_L)$, $|\boldsymbol{u}| = \sqrt{u_1^2 + \cdots + u_L^2}$ and the matrices $\boldsymbol{E}, \boldsymbol{E}^\perp$ are given by

$$\boldsymbol{E}(\boldsymbol{u}) = \Big(\frac{u_i u_j}{|\boldsymbol{u}|^2}\Big)_{L\times L}, \qquad \boldsymbol{E}^\perp = \boldsymbol{I} - \boldsymbol{E}.$$

Usually d_l is considerably larger than d_t, hence we assume $d_l > d_t$.

From the analysis of [16], the definitions (2.17) and (2.23), we know that for $\boldsymbol{u}, \boldsymbol{v} \in C(\overline{\Omega_d})^L$, there holds

$$D_{\min}|\boldsymbol{\xi}|^2 \le \overline{\boldsymbol{D}}(\boldsymbol{u})\boldsymbol{\xi} \cdot \boldsymbol{\xi} \le D_{\max}|\boldsymbol{\xi}|^2, \quad \boldsymbol{\xi} \in R^L, \tag{2.24}$$

$$(\boldsymbol{D}(\boldsymbol{u}) - \boldsymbol{D}(\boldsymbol{v}))(i, j) \le (3d_l - 2d_t)|\boldsymbol{u} - \boldsymbol{v}|, \quad 1 \le i, j \le 2. \tag{2.25}$$

Before giving the suitable weak formulations of the problems (2.1)−(2.16), we introduce some useful notations.

The Sobolev space $W^{m,n}$ and $L^q(J; W^{m,n}(\Omega))$ are defined in the usual way with the usual norm $\|\cdot\|_{W^{m,n}}$ and $\|\cdot\|_{L^q(J;W^{m,n}(\Omega))}$, where $0 \le m < \infty$, $0 \le n \le \infty$, $0 \le q \le \infty$. When $n = 2$, we simply substitute $H^m(\Omega)$ for $W^{m,2}(\Omega)$ with $\|\cdot\|_{m,\Omega} = \|\cdot\|_{W^{m,2}(\Omega)}$, $|\cdot|_{m,\Omega} = |\cdot|_{W^{m,2}(\Omega)}$. In particular, when $m = 0$, we have $L^2(\Omega) = H^0(\Omega)$, with $\|\cdot\|$ for $\|\cdot\|_{0,\Omega}$. Let $(\cdot,\cdot)_\Omega$ denote $L^2(\Omega)$, $L^2(\Omega)^L$ or $L^2(\Omega)^{L\times L}$ inner product or duality pairing. Also, $\|\cdot\|_l, |\cdot|_l, l = s, d$, will be the same with Ω replaced by $\Omega_l, l = s, d$. The $L^2(\Gamma_I)$ inner product or duality pairing is denoted by $\langle\cdot,\cdot\rangle_{\Gamma_I}$.

The special vector-function space is defined by

$$\boldsymbol{H}(div;\Omega) = \{\boldsymbol{v} \in (L^2(\Omega))^L, \nabla \cdot \boldsymbol{v} \in L^2(\Omega)\}.$$

To present a variational form of the coupled problem, the spaces for the velocity, pressure and concentration are defined as follows

$$\boldsymbol{V} = \{\boldsymbol{v} \in \boldsymbol{H}(div;\Omega) : \boldsymbol{v} \in (H^1(\Omega_s))^L,\ \boldsymbol{v} = 0\ on\ \Gamma_s,\ \boldsymbol{v}\cdot\boldsymbol{n}_d = 0\ on\ \Gamma_d\}$$

equipped with the norm

$$\|\boldsymbol{v}\|_V = \left(|\boldsymbol{v}|_{1,s}^2 + \|\boldsymbol{v}\|_{0,d}^2 + \|\nabla\cdot\boldsymbol{v}\|_{0,d}^2\right)^{1/2},$$

$Q = \{q \in L^2(\Omega) : \int_\Omega q dx = 0\}$, with the norm $\|\cdot\|_Q = \|\cdot\|$, and $W = H^1(\Omega)$ with the norm $\|\cdot\|_W = \|\cdot\|_1$. Note that the vector valued functions in $\boldsymbol{V}$ have (weakly) continuous normal components on Γ_I [4].

We also consider the convection term of the concentration equation as in [33]. For $z \in W$ it is clear that

$$\begin{aligned}(\boldsymbol{u}\cdot\nabla c, z) &= -(\boldsymbol{u}c, \nabla z) - (\nabla\cdot\boldsymbol{u}c, z)\\ &= -(\boldsymbol{u}c, \nabla z) - ((q^I - q^P)c, z)_d.\end{aligned}$$

So we have

$$\begin{aligned}(\boldsymbol{u}\cdot\nabla c, z) + (q^I c, z)_d &= \frac{1}{2}(\boldsymbol{u}\cdot\nabla c, z) + \frac{1}{2}(\boldsymbol{u}\cdot\nabla c, z) + (q^I c, z)_d\\ &= \frac{1}{2}(\boldsymbol{u}\cdot\nabla c, z) - \frac{1}{2}(\boldsymbol{u}c, \nabla z) + \frac{1}{2}((q^I + q^P)c, z)_d. \qquad (2.26)\end{aligned}$$

Using (2.26), we now propose the following weak formulation of the coupled problems (2.1)–(2.16): find $\boldsymbol{u}(t) \in \boldsymbol{V}$, $p(t) \in Q$, $c(t) \in W$ such that for a.e. $t \in J$

$$(\partial_t\boldsymbol{u}, \boldsymbol{v}) + a(c;\boldsymbol{u},\boldsymbol{v}) + b(\boldsymbol{v}, p) = F(c;\boldsymbol{v}), \quad \forall \boldsymbol{v} \in \boldsymbol{V}, \qquad (2.27)$$

$$b(\boldsymbol{u}, q) = H(q), \quad \forall q \in Q, \qquad (2.28)$$

$$(\partial_t c, z)_{\overline{\phi}} + d(\boldsymbol{u}; c, z) = G(z), \quad \forall z \in W, \qquad (2.29)$$

$$(\boldsymbol{u}(0), \boldsymbol{v})_s = (\boldsymbol{u}_{s,0}, \boldsymbol{v})_s, \quad \forall \boldsymbol{v} \in \boldsymbol{V}, \qquad (2.30)$$

$$(c(0), z)_{\overline{\phi}} = (c_0, z)_{\overline{\phi}}, \quad z \in W, \qquad (2.31)$$

where

$$a(c;\boldsymbol{u},\boldsymbol{v}) = (2\mu(c)\boldsymbol{S}(\boldsymbol{u}), \boldsymbol{S}(\boldsymbol{v}))_s + \sum_{j=1}^{L-1}\langle\gamma_j\mu(c)\boldsymbol{u}_s\cdot\boldsymbol{\tau}_j, \boldsymbol{v}_s\cdot\boldsymbol{\tau}_j\rangle_{\Gamma_I} + (\lambda^{-1}(c)\boldsymbol{u}, \boldsymbol{v})_d, \qquad (2.32)$$

$$b(\boldsymbol{v}, p) = -(p, \nabla\cdot\boldsymbol{v})_\Omega, \qquad (2.33)$$

$$F(c;\boldsymbol{v}) = (\boldsymbol{f}(c), \boldsymbol{v})_s, \qquad (2.34)$$

$$H(q) = -(q^I - q^P, q)_d, \qquad (2.35)$$

$$(c, z)_{\overline{\phi}} = (\overline{\phi}c, z)_\Omega, \qquad (2.36)$$

$$d(\boldsymbol{u}; c, z) = (\overline{\boldsymbol{D}}(\boldsymbol{u})\nabla c, \nabla z)_\Omega + \frac{1}{2}(\boldsymbol{u}\cdot\nabla c, z) - \frac{1}{2}(\boldsymbol{u}c, \nabla z) + \frac{1}{2}((q^I + q^P)c, z)_d, \qquad (2.37)$$

$$G(z) = (q^I c^I, z)_d, \qquad (2.38)$$

$$\overline{\phi} = \begin{cases} 1, & in \quad \Omega_s, \\ \phi, & in \quad \Omega_d. \end{cases}$$

Interface conditions (2.7)–(2.9) and (2.11) are posed weakly in the above variational form, while (2.10) is treated as an essential condition. Due to (2.18), $(\cdot,\cdot)_{\overline{\phi}}$ is an equivalent scalar product on $L^2(\Omega)$ and $\|c\|_{\overline{\phi}} = (c,c)_{\overline{\phi}}^{1/2}$ defines an equivalent norm on $L^2(\Omega)$.

3. Finite element discretization and multiple time step method

In this section, we consider the finite element discretization of the coupled problem and propose a multiple time step method. We will use the nonconforming Crouzeix-Raviart piecewise linear finite element approximation for velocity, piecewise constant approximation for pressure, and continuous piecewise linear polynomial approximation for concentration, the penalizing term is the same as [32]. It should be noted that, the time step for velocity and pressure is different from concentration, which will increase the computing efficiency. The existence and uniqueness of a finite element solution of the discrete problem will also be established in this section. It should be mentioned that the existence and uniqueness is unconditionally satisfied, which benefit from using Crouzeix-Raviart finite element method to solve coupling problems.

Let $\mathscr{T}_h$ be a family of triangulations of Ω with nondegenerate elements, that means Ω is completely triangulated into triangles($L = 2$) or tetrahedron ($L = 3$). For any $T \in \mathscr{T}_h$, we denote the diameter of T as h_T, $h = \max_{T\in\mathscr{T}_h} h_T$ and the diameter of the sphere inscribed in T as ρ_T. $\mathscr{T}_h$ is regular in the sense of Ciarlet [13], that is, there exists a constant σ independent of h and T such that

$$\sigma_T = \frac{h_T}{\rho_T} \le \sigma, \quad \forall T \in \mathscr{T}_h.$$

Remark 3.1. *Ω is completely triangulated into triangles ($L = 2$) or tetrahedron ($L = 3$), so each interface and boundary are assumed to be polygonal. This approximation makes it impossible for the numerical discrete scheme to fully match Figure 1. Figure 1 is intended to demonstrate the general model that satisfies the Eqs (2.1)–(2.16). Polygonal simplification was carried out during discretization to facilitate approximate calculation and solution. Further research is needed on the approximation of general smooth curves.*

Assume each element $T \in \mathscr{T}_h$ is in either Ω_s or Ω_d, denote $\mathscr{T}_h^s$ and $\mathscr{T}_h^d$ as the corresponding induced triangulations of Ω_s and Ω_d. For any $T \in \mathscr{T}_h$, $\mathcal{E}(T)$ is denoted as the set of its edges ($L = 2$) or face ($L = 3$), and set $\mathcal{E}_h = \bigcup_{T\in\mathscr{T}_h} \mathcal{E}(T)$. We split $\mathcal{E}_h$ into the following form

$$\mathcal{E}_h = \mathcal{E}_h(\Omega_s^+) \cup \mathcal{E}_h(\Omega_d) \cup \mathcal{E}_h(\partial\Omega_d), \tag{3.1}$$

where $\Omega_s^+ = \Omega_s \cup \Gamma_s$, $\mathcal{E}_h(\mathscr{S}) = \{E \in \mathcal{E}_h : E \subset \mathscr{S}\}$.

With every edge $E \in \mathcal{E}_h$ we associate a unit vector $\boldsymbol{n}_E$ such that $\boldsymbol{n}_E$ is orthogonal to E. For any $E \in \mathcal{E}_h$ and any piecewise continuous function φ, we denote by $[\varphi]_E$ the jump of φ across E in the direction $\boldsymbol{n}_E$:

$$[\varphi]_E(x) = \begin{cases} \lim\limits_{t\to0^+} \varphi(x + t\boldsymbol{n}_E) - \lim\limits_{t\to0^+} \varphi(x - t\boldsymbol{n}_E), & if\ E \not\subset \partial\Omega, \\ -\lim\limits_{t\to0^+} \varphi(x - t\boldsymbol{n}_E), & if\ E \subset \partial\Omega. \end{cases} \tag{3.2}$$

Define the nonconforming Crouzeix-Raviart piecewise linear finite element space

$$\begin{aligned}\boldsymbol{V}_h = \Big\{ & \boldsymbol{v}_h : \boldsymbol{v}_h|_T \in (P_1(T))^L, \quad \forall T \in \mathscr{T}_h, \\ & \int_E [\boldsymbol{v}_h]_E ds = 0, \quad \forall E \in \mathcal{E}_h(\Omega_s^+) \cup \mathcal{E}_h(\Omega_d), \\ & \int_E [\boldsymbol{v}_E \cdot \boldsymbol{n}_E]_E ds = 0, \quad \forall E \in \mathcal{E}_h(\partial\Omega_d) \Big\},\end{aligned} \tag{3.3}$$

and piecewise constant function space

$$Q_h = \left\{ q_h : q_h|_T \in P_0(T),\ \forall T \in \mathscr{T}_h,\ \int_\Omega q_h dx = 0 \right\}, \tag{3.4}$$

where $P_m(T)$ is the space of the restrictions to T of all polynomials of degree less than or equal to m. And define the classical Galerkin finite element space

$$W_h = \{z_h : z_h \in C^0(\Omega), z_h|_T \in P^1(T), \forall T \in \mathscr{T}_h\}, \tag{3.5}$$

it is clear that $W_h \subset W$.

Denote the operator $div_h \in \mathscr{L}(\boldsymbol{V}_h, Q_h) \cap \mathscr{L}(\boldsymbol{V}, Q)$ by $div_h \boldsymbol{v}|_T = \nabla \cdot \boldsymbol{v}|_T,\ \forall T \in \mathscr{T}_h$. Then define some bilinear forms

$$\begin{aligned} a_h(c; \boldsymbol{u}, \boldsymbol{v}) = & \sum_{T \in \mathscr{T}_h^s} (2\mu(c)\boldsymbol{S}(\boldsymbol{u}), \boldsymbol{S}(\boldsymbol{v}))_T + \sum_{j=1}^{L-1} \langle \gamma_j \mu(c) \boldsymbol{u}_s \cdot \boldsymbol{\tau}_j, \boldsymbol{v}_s \cdot \boldsymbol{\tau}_j \rangle_{\Gamma_I} \\ & + \sum_{T \in \mathscr{T}_h^d} (\lambda^{-1}(c)\boldsymbol{u}, \boldsymbol{v})_T, \quad \forall \boldsymbol{u}, \boldsymbol{v} \in \boldsymbol{V} + \boldsymbol{V}_h, \end{aligned}$$

$$b_h(\boldsymbol{v}, p) = -(p, div_h \boldsymbol{v})_\Omega, \quad \forall \boldsymbol{v} \in \boldsymbol{V} + \boldsymbol{V}_h, p \in Q,$$

and penalty term

$$j(\boldsymbol{u}, \boldsymbol{v}) = j_{\Omega_s^+}(\boldsymbol{u}, \boldsymbol{v}) + j_{\Omega_d}(\boldsymbol{u}, \boldsymbol{v}) + j_{\partial\Omega_d}(\boldsymbol{u}, \boldsymbol{v}) \quad \forall \boldsymbol{u}, \boldsymbol{v} \in \boldsymbol{V} + \boldsymbol{V}_h, \tag{3.6}$$

with

$$\begin{cases} j_{\Omega_s^+}(\boldsymbol{u}, \boldsymbol{v}) = (1 + 2\mu_{\min}) \displaystyle\sum_{E \in \mathcal{E}_h(\Omega_s^+)} \int_E \frac{1}{h_E} [\boldsymbol{u}]_E \cdot [\boldsymbol{v}]_E ds, \\ j_{\Omega_d}(\boldsymbol{u}, \boldsymbol{v}) = \displaystyle\sum_{E \in \mathcal{E}_h(\Omega_d)} \int_E \frac{1}{h_E} [\boldsymbol{u}]_E \cdot [\boldsymbol{v}]_E ds, \\ j_{\partial\Omega_d}(\boldsymbol{u}, \boldsymbol{v}) = \displaystyle\sum_{E \in \mathcal{E}_h(\partial\Omega_d)} \int_E \frac{1}{h_E} [\boldsymbol{u} \cdot \boldsymbol{n}_E]_E \cdot [\boldsymbol{v} \cdot \boldsymbol{n}_E]_E ds, \end{cases} \tag{3.7}$$

where $(\cdot, \cdot)_T$ is $L^2(T)$, $(L^2(T))^L$ or $(L^2(T))^{L\times L}$ inner product or duality pairing, h_E is the length ($L = 2$) or the diameter ($L = 3$) of E. Note that each edge ($L = 2$) or face ($L = 3$) of $\mathcal{E}_h$ only correlates with one jump term of $j(\boldsymbol{u}, \boldsymbol{v})$.

Now we give the numerical scheme with different time steps. Assume that to each time level τ_m for concentration, there exists a time level t_{n_m} for velocity and pressure. For simplicity, define uniform time levels as

$$t_n = n\Delta t,\ n = 0, 1, 2, \ldots, N, \quad \tau_m = m\Delta\tau,\ m = 0, 1, 2, \ldots, M, \quad \Delta\tau = r \cdot \Delta t,$$

where $\Delta t = \dfrac{T_1}{N}$, $\Delta\tau = \dfrac{T_1}{M}$, and $N = r \cdot M$, which means $n_m = r \cdot m$. Here r is the ratio of the different time steps, we will give the relationship between the value of the ratio and the physical parameters of the equations in next section.

The relationship of the time steps is given in Figure 2.

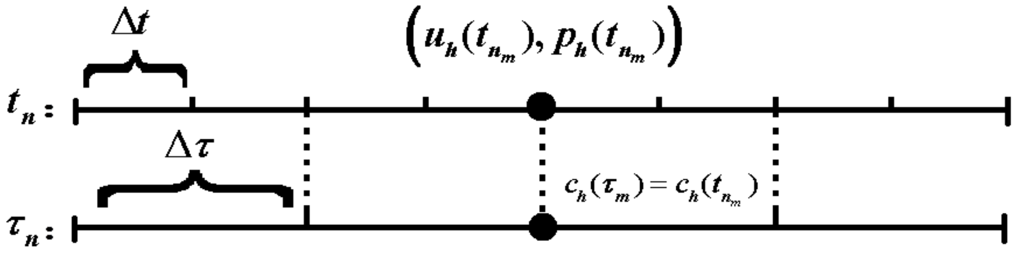

Figure 2. Relationship of the time steps.

Let

$$\boldsymbol{u}_h^n = \boldsymbol{u}_h(t_n), \quad p_h^n = p_h(t_n), \quad C_h^m = c_h^{n_m} = c_h(t_{n_m}) = c_h(\tau_m),$$

$$d_t\boldsymbol{u}_h^{n+1} = \frac{(\boldsymbol{u}_h^{n+1} - \boldsymbol{u}_h^n)}{\Delta t}, \quad d_\tau C_h^{m+1} = \frac{(C_h^{m+1} - C_h^m)}{\Delta\tau} = \frac{(c_h^{n_{m+1}} - c_h^{n_m})}{\Delta\tau},$$

and

$$A_h(C_h^m; \boldsymbol{u}_h^{n+1}, \boldsymbol{v}_h) = a_h(C_h^m; \boldsymbol{u}_h^{n+1}, \boldsymbol{v}_h) + j(\boldsymbol{u}_h^{n+1}, \boldsymbol{v}_h).$$

Set the initial approximations as

$$\boldsymbol{u}_{h,s}^0 = \boldsymbol{u}_{h,s}^{n_0} = \boldsymbol{r}_h\boldsymbol{u}_{s,0}, \quad C_h^0 = c_h^0 = \Xi_h c_0,$$

where the operators $\boldsymbol{r}_h$ and Ξ_h will be defined in (3.16) and (4.3), the numerical algorithm of the fully discrete finite element scheme with different time steps is proposed as follows:

$$\begin{aligned}
\boldsymbol{Algorithm}^*: \quad & for\ m = 0 : M \\
& \quad for\ n = n_m : n_{m+1} - 1 \\
& \quad\quad Find\ (\boldsymbol{u}_h^{n+1}, p_h^{n+1}) \in V_h \times Q_h,\ such\ that \\
& \quad\quad\quad (d_t\boldsymbol{u}_h^{n+1}, \boldsymbol{v}_h)_s + A_h(\overline{C}_h^m; \boldsymbol{u}_h^{n+1}, \boldsymbol{v}_h) \\
& \quad\quad\quad\quad + b_h(\boldsymbol{v}_h, p_h^{n+1}) = F(\overline{C}_h^m; \boldsymbol{v}_h), \quad \forall \boldsymbol{v}_h \in \boldsymbol{V}_h, && (3.8) \\
& \quad\quad\quad b_h(\boldsymbol{u}_h^{n+1}, q_h) = H(q_h), \quad \forall q_h \in Q_h, && (3.9) \\
& \quad end \\
& \quad Take\ \boldsymbol{U}_h^m = \frac{1}{r}\sum_{i=n_m}^{n_{m+1}-1} \boldsymbol{u}_h^{i+1} \\
& \quad Find\ C_h^{m+1} \in W_h,\ such\ that \\
& \quad\quad (d_\tau C_h^{m+1}, z_h)_{\overline{\phi}} + d(\boldsymbol{U}_h^m; C_h^{m+1}, z_h) = G(z_h),\ \forall z_h \in W_h && (3.10) \\
& end
\end{aligned}$$

Here $\overline{C}_h^m = \min\{1, \max\{0, C_h^m\}\} \in [0, 1]$. Since $c \in [0, 1]$, so it is clear that

$$|\overline{C}_h^m - c^m| \leq |C_h^m - c^m|. \tag{3.11}$$

Each algebraic system of numerical schemes (3.8)–(3.10) in the numerical algorithm is linear. And the time step for velocity and pressure is different from concentration, which depending on the ratio r, so we can choose appropriate r to improve computing efficiency.

Define the norm of $\boldsymbol{V}_h$:

$$\|\boldsymbol{v}\|_h = \left(\sum_{T \in \mathcal{T}_h^s} |\boldsymbol{v}|_{1,T}^2 + \sum_{j=1}^{L-1} \langle \boldsymbol{v}_s \cdot \boldsymbol{\tau}_j, \boldsymbol{v}_s \cdot \boldsymbol{\tau}_j \rangle_{\Gamma_I} + \|\boldsymbol{v}\|_{0,d}^2 + \|div_h \boldsymbol{v}\|_{0,d}^2 + j(\boldsymbol{v}, \boldsymbol{v}) \right)^{1/2}, \tag{3.12}$$

and the space Q_h is equipped with the norm $\|\cdot\|$.

Then giving the definition of $\boldsymbol{Z}_h$, which is the subspace of $\boldsymbol{V}_h$:

$$\boldsymbol{Z}_h = \{\boldsymbol{v}_h \in \boldsymbol{V}_h : b_h(\boldsymbol{v}_h, q_h) = 0, \quad \forall q_h \in Q_h\},$$

we have the following lemma.

Lemma 3.1. *if $\boldsymbol{v}_h \in \boldsymbol{Z}_h$, then $div_h \boldsymbol{v}_h = 0$.*

Proof. Since $div_h \boldsymbol{v}_h \in Q_h$ for $\boldsymbol{v}_h \in \boldsymbol{V}_h$, if $\boldsymbol{v}_h \in Z_h$, take $q_h = div_h \boldsymbol{v}_h$, we have $(div_h \boldsymbol{v}_h, div_h \boldsymbol{v}_h)_\Omega = 0$, the lemma follows. □

Lemma 3.2. *The bilinear form $A_h(\cdot; \cdot, \cdot)$ is coercive on Z_h: there is a positive constant $\alpha > 0$ such that*

$$A_h(c_h; \boldsymbol{v}_h, \boldsymbol{v}_h) \geq \alpha \|\boldsymbol{v}_h\|_h^2, \quad \forall \boldsymbol{v}_h \in Z_h, \tag{3.13}$$

where $\alpha \propto \dfrac{\mu_{\min}}{k_{\max}}$ depends on σ, and is independent of h, Δt and $\Delta\tau$.

Proof. Follow Lemma 3.1, inequality (2.21) and the Korn's inequality for piecewise H^1 vector fields [3], we have

$$\begin{aligned}\sum_{T \in \mathcal{T}_h^s} (2\mu(c_h)\boldsymbol{S}(\boldsymbol{v}_h), \boldsymbol{S}(\boldsymbol{v}_h))_T + j_{\Omega_s^+}(\boldsymbol{v}_h, \boldsymbol{v}_h) &\geq 2\mu_* \sum_{T \in \mathcal{T}_h^s} (\boldsymbol{S}(\boldsymbol{v}_h), \boldsymbol{S}(\boldsymbol{v}_h))_T + j_{\Omega_s^+}(\boldsymbol{v}_h, \boldsymbol{v}_h) \\ &\geq C \sum_{T \in \mathcal{T}_h^s} |\boldsymbol{v}_h|_{1,T}^2,\end{aligned}$$

where C is a positive constant which depends only on σ and $\mu_{\min}$. Since $\gamma_j = \alpha_1/\sqrt{k_j}$ and follow inequality (2.22), we have $\alpha \propto \dfrac{\mu_{\min}}{k_{\max}}$. □

Lemma 3.3. *The bilinear forms $A_h(\cdot; \cdot, \cdot)$ and $b_h(\cdot, \cdot)$ are Bounded in $\boldsymbol{V}_h + \boldsymbol{V}$: there is a positive constant A such that*

$$|A_h(c_h; \boldsymbol{u}_h, \boldsymbol{v}_h)| \leq A\|\boldsymbol{u}_h\|_h \|\boldsymbol{v}_h\|_h, \quad \forall \boldsymbol{u}_h, \boldsymbol{v}_h \in \boldsymbol{V}_h + \boldsymbol{V}, \tag{3.14}$$

$$|b_h(\boldsymbol{v}_h, q_h)| \leq \sqrt{L}\|\boldsymbol{v}_h\|_h \|q_h\|, \quad \forall \boldsymbol{v}_h \in \boldsymbol{V}_h + \boldsymbol{V}, p_h \in Q_h, \tag{3.15}$$

where $A \propto \dfrac{\mu_{\max}}{k_{\min}} + \mu_{\max}$ is independent of h, Δt and $\Delta\tau$.

Proof. The lemma follows from Hölder inequality. □

Define the space

$$X = \{\boldsymbol{v} \in \boldsymbol{V} : \boldsymbol{v}_d \in (H^1(\Omega_d))^L\},$$

we give the definition of the Crouzeix-Raviart interpolation operator $\boldsymbol{r}_h : \boldsymbol{X} \to \boldsymbol{V}_h,\ \forall t \in J$

$$\int_E (\boldsymbol{r}_h \boldsymbol{v}(t))_l ds = \int_E \boldsymbol{v}(t)_l ds, \quad \forall E \in \mathcal{E}_h, E \subset \overline{\Omega}_l, \quad l = s \text{ or } d. \tag{3.16}$$

From the interpolation theory for $\boldsymbol{r}_h$ [14], we have the standard Bramble-Hilbert estimation

$$\|\boldsymbol{r}_h \boldsymbol{v} - \boldsymbol{v}\|_{s_1,T} \leq R h^{s_2 - s_1} |\boldsymbol{v}|_{s_2,T}, \quad 0 \leq s_1 \leq 1 \leq s_2 \leq 2, \tag{3.17}$$

where R is independent of h.

From [20] and the definition of $\boldsymbol{r}_h \boldsymbol{v}$, we know that the discrete inf-sup condition is satisfied. The proof can be found in [33].

Lemma 3.4. *There exists a constant $\beta > 0$ depending on σ, $\mu_{\min}$ such that*

$$\inf_{p_h \in Q_h} \sup_{\boldsymbol{v}_h \in \boldsymbol{V}_h} \frac{b_h(\boldsymbol{v}_h, p_h)}{\|p_h\| \|\boldsymbol{v}_h\|_h} \geq \beta. \tag{3.18}$$

Lemma 3.5. *The nonlinear form $d(\cdot;\cdot,\cdot)$ is positive definite, that is*

$$d(\boldsymbol{u}; z, z) \geq \boldsymbol{D}_{\min}(\nabla z, \nabla z)_\Omega + \frac{1}{2}((q^I + q^P)z, z)_d, \qquad \forall z \in W. \tag{3.19}$$

Proof. From the definition (2.36), we have

$$\begin{aligned} d(\boldsymbol{u}; z, z) &= (\overline{\boldsymbol{D}}(\boldsymbol{u})\nabla z, \nabla z)_\Omega + \frac{1}{2}(\boldsymbol{u} \cdot \nabla z, z) - \frac{1}{2}(\boldsymbol{u} z, \nabla z) + \frac{1}{2}((q^I + q^P)z, z)_d \\ &= (\overline{\boldsymbol{D}}(\boldsymbol{u})\nabla z, \nabla z)_\Omega + \frac{1}{2}((q^I + q^P)z, z)_d \\ &\geq (D_{\min} \nabla z, \nabla z)_\Omega + \frac{1}{2}((q^I + q^P)z, z)_d, \qquad \forall z \in W. \end{aligned}$$

proof of positive definiteness of $d(;,)$. □

From Lemmas 3.2–3.4 and the abstract theory of mixed problem [4, 21], we derive the existence and uniqueness of velocity $\boldsymbol{u}$ and pressure p in both free region Ω_s and porous medium domain Ω_d. From Lemma 3.5 and the fact that the numerical scheme (3.10) is linear, we can also get the existence and uniqueness of concentration c. Thus we drive the existence and uniqueness of the the fully discrete finite element scheme with different time steps.

Theorem 3.2. *There exists unique solution $(\boldsymbol{u}_h^n, p_h^n) \in \boldsymbol{V}_h \times Q_h$, $n = 1, 2, \ldots, N$, and $C_h^m \in W_h$, $m = 1, 2, \ldots, M$ satisfying the numerical schemes (3.8)–(3.10) in **Algorithm***.*

4. Error estimates

In this section, we derive the error estimates for $\boldsymbol{Algorithm}^*$ and the relationship between the value of r and the physical parameters of the equations. We first define two projection operators and give corresponding estimation.

Define the projection operator $\Pi_h : Q \rightarrow Q_h,\ \forall t \in J$ by

$$\int_T (\Pi_h q(t) - q(t))dx = 0, \quad \forall T \in \mathscr{T}_h, \tag{4.1}$$

then

$$\|p(t) - \Pi_h p(t)\|_{0,T} = \min_{q(t) \in P_h(T)} \|p(t) - q(t)\|_{0,T} \leq Ch|p(t)|_{1,T}, \quad \forall T \in \mathscr{T}_h,$$

with P depending only on σ and L, so that

$$\|p(t) - \Pi_h p(t)\| \leq Ph(|p(t)|_{1,s} + |p(t)|_{1,d}). \tag{4.2}$$

Define the elliptic projection operator $\Xi_h : W \rightarrow W_h,\ \forall t \in J$ by (one can also find similar definition in [16, 40])

$$(\overline{\boldsymbol{D}}(\boldsymbol{u})\nabla(c(t) - \Xi_h c(t)), \nabla z_h) + \frac{1}{2}(\boldsymbol{u} \cdot \nabla(c(t) - \Xi_h c(t)), z_h) - \frac{1}{2}(\boldsymbol{u}(c(t) - \Xi_h c(t)), \nabla z_h)$$
$$+\frac{1}{2}((1 + q^I + q^P)(c(t) - \Xi_h c(t)), z_h)_d = 0, \quad \forall z_h \in W_h. \tag{4.3}$$

From the theory of finite element methods for elliptic problem, when c is sufficiently smooth, there hold

$$\|c(t) - \Xi_h c(t)\|_{L^2(\Omega)} + h\|\nabla(c(t) - \Xi_h c(t))\|_{L^2(\Omega)} \leq Ch\|c(t)\|_{H^1(\Omega)}, \tag{4.4}$$

$$\|\partial_t(c(t) - \Xi_h c(t))\|_{L^2(\Omega)} \leq Ch\left(\|c(t)\|_{H^1(\Omega)} + \|\partial_t c(t)\|_{H^1(\Omega)}\right), \tag{4.5}$$

$$\|\Xi_h c(t)\|_{W^{1,\infty}(\Omega)} \leq C_c, \tag{4.6}$$

where the constants C and C_c are independent of h.

From the trace theorem, we have

$$\|\varphi\|_{L^2(\Gamma_I)} \leq C\|\varphi\|_{1,s} \quad \forall \varphi \in H^1(\Omega_s), \tag{4.7}$$

and from [13], the following approximation property satisfied

$$\inf_{z \in W_h} \|\varphi - z\|_{W^{1,n}(\Omega)} \leq Ch(\|\varphi\|_{W^{2,n}(\Omega_s)} + \|\varphi\|_{W^{2,n}(\Omega_d)}), \tag{4.8}$$

where $n = 2, \infty$, $\varphi \in U^{2,n} = \left\{\varphi \in W : \varphi_s \in W^{2,n}(\Omega_s), \varphi_d \in W^{2,n}(\Omega_d)\right\}$.

For estimating the approximation error, we assume that the exact solutions satisfy the following smoothness conditions:

$$c \in L^\infty(J; H^1(\Omega)) \cap H^1(J; H^1(\Omega)) \cap L^\infty(J; W^{1,\infty}(\Omega)) \cap H^2(J; L^2(\Omega)), \tag{4.9}$$

$$\boldsymbol{u} \in W^{1,\infty}(J; H^2(\Omega_s)^L \cup H^2(\Omega_d)^L) \cap H^2(J; L^2(\Omega_s)^L \cup L^2(\Omega_d)^L) \cap H^1(J; H^1(\Omega_s)^L), \tag{4.10}$$

$$p \in W^{1,\infty}(J; H^1(\Omega_s) \cup H^1(\Omega_d)). \tag{4.11}$$

Remark 4.1. *The assumptions (4.9)–(4.11) of smoothness for exact solutions may not be sufficient for some special practical problems, but they are essential for error estimation analysis. Studying error estimation analysis approach that satisfy low smoothness of exact solutions will be our future research work.*

The smoothness assumption of $\boldsymbol{u}$ implies $j(\boldsymbol{u}, \boldsymbol{v}_h) = 0$, thus

$$A_h(\boldsymbol{u}, \boldsymbol{v}_h) = a_h(\boldsymbol{u}, \boldsymbol{v}_h), \quad \boldsymbol{v}_h \in V_h. \tag{4.12}$$

At a certain time point $n, n = 1, 2, \ldots, N$, let Eqs (2.1) and (2.4) do inner product with $\boldsymbol{v}_h \in V_h$ respectively, and add up the results. By using Green's formula on each $T \in \mathscr{T}_h$, the interface conditions (2.8), (2.9) and Eq (4.12), we obtain

$$\begin{aligned}
&(\partial_t \boldsymbol{u}^{n+1}, \boldsymbol{v}_h)_s + A_h(c^{n+1}; \boldsymbol{u}^{n+1}, \boldsymbol{v}_h) + b_h(\boldsymbol{v}_h, p^{n+1}) - F(c^{n+1}; \boldsymbol{v}_h) \\
&= - \sum_{E \in \mathcal{E}_h(\Omega_s^+)} \int_E 2\mu(c^{n+1}) \boldsymbol{n}_E \cdot \boldsymbol{S}(\boldsymbol{u}^{n+1}) \cdot [\boldsymbol{v}_h]_E ds + \sum_{E \in \mathcal{E}_h(\Omega_s^+ \cup \Omega_d)} \int_E p^{n+1} [\boldsymbol{v}_h \cdot \boldsymbol{n}_E]_E ds \\
&\quad + \sum_{E \in \mathcal{E}_h(\partial \Omega_d)} \int_E p_d^{n+1} [\boldsymbol{v}_h \cdot \boldsymbol{n}_E]_E ds, \quad \forall \boldsymbol{v}_h \in V_h,
\end{aligned} \tag{4.13}$$

and let Eqs (2.2) and (2.5) do inner product with $q_h \in Q_h$ respectively, we obtain

$$b_h(\boldsymbol{u}^{n+1}, q_h) = H(q_h), \quad \forall q_h \in Q_h. \tag{4.14}$$

Split the error as

$$\boldsymbol{u} - \boldsymbol{u}_h = \boldsymbol{u} - \boldsymbol{r}_h \boldsymbol{u} + \boldsymbol{r}_h \boldsymbol{u} - \boldsymbol{u}_h = \epsilon_{\boldsymbol{u}} + e_{\boldsymbol{u},h},$$

$$c - c_h = c - \Xi_h c + \Xi_h c - c_h = \epsilon_c + e_{c,h},$$

then subtract (4.13) and (4.14) from (3.8) and (3.9), respectively, we can obtain the following equations by inserting $\boldsymbol{r}_h \boldsymbol{u}$ and $\Pi_h p$

$$\begin{aligned}
&(d_t e_{\boldsymbol{u},h}^{n+1}, \boldsymbol{v}_h)_s + A_h(\overline{C}_h^m; e_{\boldsymbol{u},h}^{n+1}, \boldsymbol{v}_h) + b_h(\boldsymbol{v}_h, \Pi_h p^{n+1} - p_h^{n+1}) \\
&= - (\partial_t \boldsymbol{u}^{n+1} - d_t \boldsymbol{u}^{n+1}, \boldsymbol{v}_h)_s - (d_t \epsilon_{\boldsymbol{u}}^{n+1}, \boldsymbol{v}_h)_s - (A_h(c^{n+1}; \boldsymbol{u}^{n+1}, \boldsymbol{v}_h) - A_h(\overline{C}_h^m; \boldsymbol{u}^{n+1}, \boldsymbol{v}_h)) \\
&\quad - A_h(\overline{C}_h^m; \epsilon_{\boldsymbol{u}}^{n+1}, \boldsymbol{v}_h) - b_h(\boldsymbol{v}_h, p^{n+1} - \Pi_h p^{n+1}) + (F(c^{n+1}; \boldsymbol{v}_h) - F(\overline{C}_h^m; \boldsymbol{v}_h)) \\
&\quad + \Big(- \sum_{E \in \mathcal{E}_h(\Omega_s^+)} \int_E 2\mu(c^{n+1}) \boldsymbol{n}_E \cdot \boldsymbol{S}(\boldsymbol{u}^{n+1}) \cdot [\boldsymbol{v}_h]_E ds + \sum_{E \in \mathcal{E}_h(\Omega_s^+ \cup \Omega_d)} \int_E p^{n+1} [\boldsymbol{v}_h \cdot \boldsymbol{n}_E]_E ds \\
&\quad + \sum_{E \in \mathcal{E}_h(\partial \Omega_d)} \int_E p_d^{n+1} [\boldsymbol{v}_h \cdot \boldsymbol{n}_E]_E ds \Big), \quad \forall \boldsymbol{v}_h \in V_h,
\end{aligned} \tag{4.15}$$

$$b_h(e_{\boldsymbol{u},h}^{n+1}, q_h) = 0, \quad \forall q_h \in Q_h, \tag{4.16}$$

where (4.16) is obtained from the definition (3.16).

Lemma 4.1. *Suppose that the analytical solution satisfies properties (4.9)–(4.11), then there exists a positive constant $\hat{C}_1$ independent of h, Δt and $\Delta\tau$, and exists a positive constant $\hat{C}_2$ independent of h, Δt, $\Delta\tau$, and independent of physical parameters $\mu_{\max}$, $\mu_{\min}$, $k_{\min}$ and $k_{\max}$, such that for* $0 \leq l \leq M-1$,

$$\|\boldsymbol{u}^{n_{l+1}} - \boldsymbol{u}_h^{n_{l+1}}\|_s^2 + \alpha\Delta t \sum_{n=0}^{n_{l+1}-1} \|\boldsymbol{u}^{n+1} - \boldsymbol{u}_h^{n+1}\|_h^2 \leq \hat{C}_1\Big(h^2 + \Delta\tau \sum_{m=0}^{l}(\|c^{n_m} - C_h^m\|^2 + |c^{n_m} - C_h^m|_{1,s}^2)\Big)$$
$$+ \hat{C}_2(\frac{1}{\alpha} + \frac{1}{\alpha k_{\min}^2})\Big((\Delta t)^2 + (\Delta\tau)^2\Big). \tag{4.17}$$

Proof. Taking $\boldsymbol{v}_h = 2\Delta t e_{\boldsymbol{u},h}^{n+1}$ in (4.15), and combining with (4.16), we have

$$\begin{aligned}
&2(e_{\boldsymbol{u},h}^{n+1} - e_{\boldsymbol{u},h}^{n}, e_{\boldsymbol{u},h}^{n+1})_s + 2\Delta t A_h(\overline{C}_h^m; e_{\boldsymbol{u},h}^{n+1}, e_{\boldsymbol{u},h}^{n+1})\\
=& - 2\Delta t(\partial_t \boldsymbol{u}^{n+1} - d_t\boldsymbol{u}^{n+1}, e_{\boldsymbol{u},h}^{n+1})_s - 2\Delta t(d_t\epsilon_{\boldsymbol{u}}^{n+1}, e_{\boldsymbol{u},h}^{n+1})_s\\
&- 2\Delta t(A_h(c^{n+1}; \boldsymbol{u}^{n+1}, e_{\boldsymbol{u},h}^{n+1}) - A_h(\overline{C}_h^m; \boldsymbol{u}^{n+1}, e_{\boldsymbol{u},h}^{n+1})) - A_h(\overline{C}_h^m; \epsilon_{\boldsymbol{u}}^{n+1}, 2\Delta t e_{\boldsymbol{u},h}^{n+1})\\
&- b_h(2\Delta t e_{\boldsymbol{u},h}^{n+1}, p^{n+1} - \Pi_h p^{n+1}) + 2\Delta t(F(c^{n+1}; e_{\boldsymbol{u},h}^{n+1}) - F(\overline{C}_h^m; e_{\boldsymbol{u},h}^{n+1}))\\
&+ 2\Delta t\Big(- \sum_{E\in\mathcal{E}_h(\Omega_s^+)} \int_E 2\mu(c^{n+1})\boldsymbol{n}_E \cdot \boldsymbol{S}(\boldsymbol{u}^{n+1}) \cdot [e_{\boldsymbol{u},h}^{n+1}]_E ds + \sum_{E\in\mathcal{E}_h(\Omega_s^+\cup\Omega_d)} \int_E p^{n+1}[e_{\boldsymbol{u},h}^{n+1} \cdot \boldsymbol{n}_E]_E ds\\
&+ \sum_{E\in\mathcal{E}_h(\partial\Omega_d)} \int_E p_d^{n+1}[e_{\boldsymbol{u},h}^{n+1} \cdot \boldsymbol{n}_E]_E ds\Big).
\end{aligned} \tag{4.18}$$

As inner product has the following property

$$2(\gamma_1, \gamma_1 - \gamma_2) = (\gamma_1, \gamma_1) - (\gamma_2, \gamma_2) + (\gamma_1 - \gamma_2, \gamma_1 - \gamma_2) \geq (\gamma_1, \gamma_1) - (\gamma_2, \gamma_2), \tag{4.19}$$

using (3.13), (4.19) and summing over (4.18) with $n = n_m, n_m + 1, \ldots, n_{m+1} - 1$, we obtain

$$\begin{aligned}
&\|e_{\boldsymbol{u},h}^{n_{m+1}}\|_s^2 - \|e_{\boldsymbol{u},h}^{n_m}\|_s^2 + 2\alpha\Delta t \sum_{n=n_m}^{n_{m+1}-1} \|e_{\boldsymbol{u},h}^{n+1}\|_h^2\\
\leq& - 2\Delta t \sum_{n=n_m}^{n_{m+1}-1} (\partial_t \boldsymbol{u}^{n+1} - d_t\boldsymbol{u}^{n+1}, e_{\boldsymbol{u},h}^{n+1})_s - 2\Delta t \sum_{n=n_m}^{n_{m+1}-1} (d_t\epsilon_{\boldsymbol{u}}^{n+1}, e_{\boldsymbol{u},h}^{n+1})_s\\
&- 2\Delta t \sum_{n=n_m}^{n_{m+1}-1} (A_h(c^{n+1}; \boldsymbol{u}^{n+1}, e_{\boldsymbol{u},h}^{n+1}) - A_h(\overline{C}_h^m; \boldsymbol{u}^{n+1}, e_{\boldsymbol{u},h}^{n+1})) - \sum_{n=n_m}^{n_{m+1}-1} A_h(\overline{C}_h^m; \epsilon_{\boldsymbol{u}}^{n+1}, 2\Delta t e_{\boldsymbol{u},h}^{n+1})\\
&- \sum_{n=n_m}^{n_{m+1}-1} b_h(2\Delta t e_{\boldsymbol{u},h}^{n+1}, p^{n+1} - \Pi_h p^{n+1}) + 2\Delta t \sum_{n=n_m}^{n_{m+1}-1} (F(c^{n+1}; e_{\boldsymbol{u},h}^{n+1}) - F(\overline{C}_h^m; e_{\boldsymbol{u},h}^{n+1}))\\
&+ 2\Delta t \sum_{n=n_m}^{n_{m+1}-1} \Big(- \sum_{E\in\mathcal{E}_h(\Omega_s^+)} \int_E 2\mu(c^{n+1})\boldsymbol{n}_E \cdot \boldsymbol{S}(\boldsymbol{u}^{n+1}) \cdot [e_{\boldsymbol{u},h}^{n+1}]_E ds\\
&+ \sum_{E\in\mathcal{E}_h(\Omega_s^+\cup\Omega_d)} \int_E p^{n+1}[e_{\boldsymbol{u},h}^{n+1} \cdot \boldsymbol{n}_E]_E ds + \sum_{E\in\mathcal{E}_h(\partial\Omega_d)} \int_E p_d^{n+1}[e_{\boldsymbol{u},h}^{n+1} \cdot \boldsymbol{n}_E]_E ds\Big).\\
=&S_1 + S_2 + S_3 + S_4 + S_5 + S_6 + S_7.
\end{aligned} \tag{4.20}$$

Now we estimate the terms $S_1, S_2, \ldots, S_7$ individually by using Cauchy-Schwarz inequality.

Integrating by parts about t, we obtain

$$
\begin{aligned}
|S_1| \leq & 2\Delta t \sum_{n=n_m}^{n_{m+1}-1} |(\partial_t \boldsymbol{u}^{n+1} - d_t \boldsymbol{u}^{n+1}, e_{\boldsymbol{u},h}^{n+1})_s| \\
\leq & \frac{\alpha \Delta t}{7} \sum_{n=n_m}^{n_{m+1}-1} \|e_{\boldsymbol{u},h}^{n+1}\|_h^2 + \frac{7\Delta t}{\alpha} \sum_{n=n_m}^{n_{m+1}-1} \frac{1}{(\Delta t)^2} \int_{\Omega_s} (\int_{t_n}^{t_{n+1}} (t-t_n)\partial_t^2 \boldsymbol{u} dt)^2 dx \\
\leq & \frac{\alpha \Delta t}{7} \sum_{n=n_m}^{n_{m+1}-1} \|e_{\boldsymbol{u},h}^{n+1}\|_h^2 + \frac{7}{\alpha \Delta t} \sum_{n=n_m}^{n_{m+1}-1} \int_{\Omega_s} \int_{t_n}^{t_{n+1}} (\partial_t^2 \boldsymbol{u})^2 dt \int_{t_n}^{t_{n+1}} (t-t_n)^2 dt dx \\
= & \frac{\alpha \Delta t}{7} \sum_{n=n_m}^{n_{m+1}-1} \|e_{\boldsymbol{u},h}^{n+1}\|_h^2 + \frac{7(\Delta t)^2}{3\alpha} \int_{t_{n_m}}^{t_{n_{m+1}}} \|\partial_t^2 \boldsymbol{u}\|_s^2 dt,
\end{aligned}
\tag{4.21}
$$

where $\partial_t^2 \boldsymbol{u} = \partial^2 \boldsymbol{u}/\partial t^2$, and combine with (3.17), we obtain

$$
\begin{aligned}
|S_2| \leq & 2\Delta t \sum_{n=n_m}^{n_{m+1}-1} |(d_t \epsilon_{\boldsymbol{u}}^{n+1}, e_{\boldsymbol{u},h}^{n+1})| \\
\leq & \frac{\alpha \Delta t}{7} \sum_{n=n_m}^{n_{m+1}-1} \|e_{\boldsymbol{u},h}^{n+1}\|_h^2 + \frac{7\Delta t}{\alpha} \sum_{n=n_m}^{n_{m+1}-1} \frac{1}{(\Delta t)^2} \int_{\Omega_s} (\int_{t_n}^{t_{n+1}} \partial_t \epsilon_{\boldsymbol{u}} dt)^2 dx \\
\leq & \frac{\alpha \Delta t}{7} \sum_{n=n_m}^{n_{m+1}-1} \|e_{\boldsymbol{u},h}^{n+1}\|_h^2 + \frac{7}{\alpha \Delta t} \sum_{n=n_m}^{n_{m+1}-1} \int_{\Omega_s} (\int_{t_n}^{t_{n+1}} (\partial_t \epsilon_{\boldsymbol{u}})^2 dt \int_{t_n}^{t_{n+1}} 1^2 dt) dx \\
\leq & \frac{\alpha \Delta t}{7} \sum_{n=n_m}^{n_{m+1}-1} \|e_{\boldsymbol{u},h}^{n+1}\|_h^2 + \frac{7R^2 h^2}{\alpha} \int_{t_{n_m}}^{t_{n_{m+1}}} |\partial_t \boldsymbol{u}|_{1,s}^2 dt.
\end{aligned}
\tag{4.22}
$$

From (3.11), (4.7), (4.12) and the assumption that μ is Lipschitz continuous, we obtain

$$
\begin{aligned}
|S_3| \leq & 2\Delta t \sum_{n=n_m}^{n_{m+1}-1} |(A_h(c^{n+1}; \boldsymbol{u}^{n+1}, e_{\boldsymbol{u},h}^{n+1}) - A_h(\overline{C}_h^m; \boldsymbol{u}^{n+1}, e_{\boldsymbol{u},h}^{n+1}))| \\
= & 2\Delta t \sum_{n=n_m}^{n_{m+1}-1} |(a_h(c^{n+1}; \boldsymbol{u}^{n+1}, e_{\boldsymbol{u},h}^{n+1}) - a_h(\overline{C}_h^m; \boldsymbol{u}^{n+1}, e_{\boldsymbol{u},h}^{n+1}))| \\
\leq & \frac{\alpha \Delta t}{7} \sum_{n=n_m}^{n_{m+1}-1} \|e_{\boldsymbol{u},h}^{n+1}\|_h^2 + \frac{21C\Delta t}{\alpha} \sum_{n=n_m}^{n_{m+1}-1} |\mu(c^{n+1}) - \mu(\overline{C}_h^m)|_{1,s}^2 \\
& + \frac{21C\Delta t}{\alpha} \sum_{n=n_m}^{n_{m+1}-1} \|\mu(c^{n+1}) - \mu(\overline{C}_h^m)\|_s^2 + \frac{21C\Delta t}{\alpha k_{\min}^2} \sum_{n=n_m}^{n_{m+1}-1} \|\mu(c^{n+1}) - \mu(\overline{C}_h^m)\|_d^2 \\
\leq & \frac{\alpha \Delta t}{7} \sum_{n=n_m}^{n_{m+1}-1} \|e_{\boldsymbol{u},h}^{n+1}\|_h^2 + \frac{21C\mu_L^2 \Delta t}{\alpha} \sum_{n=n_m}^{n_{m+1}-1} |c^{n+1} - c_h^{n_m}|_{1,s}^2 \\
& + \frac{21C\mu_L^2 \Delta t}{\alpha} \sum_{n=n_m}^{n_{m+1}-1} \|c^{n+1} - c_h^{n_m}\|_s^2 + \frac{21C\mu_L^2 \Delta t}{\alpha k_{\min}^2} \sum_{n=n_m}^{n_{m+1}-1} \|c^{n+1} - c_h^{n_m}\|_d^2,
\end{aligned}
\tag{4.23}
$$

where C is independent of h, Δt and independent of physical parameters $\mu_{\max},\ \mu_{\min},\ k_{\min},\ k_{\max}$.

We estimate the last three items of (4.23) in turn, since for $n = n_m, \dots, n_{m+1} - 1$,

$$\|c^{n+1} - c^{n_m}\|^2 \le (\|c^{n+1} - c^n\|^2 + \|c^n - c^{n-1}\|^2 + \cdots + \|c^{n_m+1} - c^{n_m}\|^2) \le \sum_{n=n_m}^{n_{m+1}-1} \|c^{n+1} - c^n\|^2,$$

and $n_{m+1} - n_m = r$, we have

$$\sum_{n=n_m}^{n_{m+1}-1} \|c^{n+1} - c^{n_m}\|^2 \le r \sum_{n=n_m}^{n_{m+1}-1} \|c^{n+1} - c^n\|^2. \tag{4.24}$$

Thus

$$\begin{aligned}
&\frac{21C\mu_L^2\Delta t}{\alpha}\sum_{n=n_m}^{n_{m+1}-1}|c^{n+1} - c_h^{n_m}|_{1,s}^2\\
\le&\frac{21C\mu_L^2\Delta t}{\alpha}\sum_{n=n_m}^{n_{m+1}-1}(|c^{n+1} - c^{n_m}|_{1,s}^2 + |c^{n_m} - c_h^{n_m}|_{1,s}^2)\\
\le&\frac{21C\mu_L^2\Delta t}{\alpha}(r\sum_{n=n_m}^{n_{m+1}-1}|c^{n+1} - c^n|_{1,s}^2 + r|c^{n_m} - c_h^{n_m}|_{1,s}^2)\\
\le&\frac{21C\mu_L^2\Delta\tau}{\alpha}|c^{n_m} - c_h^{n_m}|_{1,s}^2 + \frac{21C\mu_L^2\Delta\tau\Delta t}{\alpha}\sum_{n=n_m}^{n_{m+1}-1}\int_{t_n}^{t_{n+1}}|\partial_t c|_{1,s}^2 dt\\
\le&\frac{21C\mu_L^2\Delta\tau}{\alpha}|c^{n_m} - c_h^{n_m}|_{1,s}^2 + \frac{21C\mu_L^2((\Delta\tau)^2 + (\Delta t)^2)}{2\alpha}\int_{t_{n_m}}^{t_{n_{m+1}}}|\partial_t c|_{1,s}^2 dt,
\end{aligned} \tag{4.25}$$

$$\begin{aligned}
&\frac{21C\mu_L^2\Delta t}{\alpha}\sum_{n=n_m}^{n_{m+1}-1}\|c^{n+1} - c_h^{n_m}\|_s^2\\
\le&\frac{21C\mu_L^2\Delta\tau}{\alpha}\|c^{n_m} - c_h^{n_m}\|_s^2 + \frac{21C\mu_L^2((\Delta\tau)^2 + (\Delta t)^2)}{2\alpha}\int_{t_{n_m}}^{t_{n_{m+1}}}\|\partial_t c\|_s^2 dt,
\end{aligned} \tag{4.26}$$

$$\begin{aligned}
&\frac{21C\mu_L^2\Delta t}{\alpha k_{\min}^2}\sum_{n=n_m}^{n_{m+1}-1}\|c^{n+1} - c_h^{n_m}\|_d^2\\
\le&\frac{21C\mu_L^2\Delta\tau}{\alpha k_{\min}^2}\|c^{n_m} - c_h^{n_m}\|_d^2 + \frac{21C\mu_L^2((\Delta\tau)^2 + (\Delta t)^2)}{2\alpha k_{\min}^2}\int_{t_{n_m}}^{t_{n_{m+1}}}\|\partial_t c\|_d^2 dt.
\end{aligned} \tag{4.27}$$

Take (4.25)−(4.27) back to (4.23), the estimate of T_3 is

$$\begin{aligned}
|S_3| \le&\frac{\alpha\Delta t}{7}\sum_{n=n_m}^{n_{m+1}-1}\|e_{\boldsymbol{u},h}^{n+1}\|_h^2 + \frac{21C\mu_L^2\Delta\tau}{\alpha}(|c^{n_m} - C_h^m|_{1,s}^2 + \|c^{n_m} - C_h^m\|_s^2 + \frac{1}{k_{\min}^2}\|c^{n_m} - C_h^m\|_d^2)\\
&+ \frac{21C\mu_L^2((\Delta\tau)^2 + (\Delta t)^2)}{2\alpha}\int_{t_{n_m}}^{t_{n_{m+1}}}(|\partial_t c|_{1,s}^2 + \|\partial_t c\|_s^2 + \frac{1}{k_{\min}^2}\|\partial_t c\|_d^2)dt.
\end{aligned} \tag{4.28}$$

From (3.14) and (3.17), we obtain

$$
\begin{aligned}
|S_4| \leq & 2\Delta t \sum_{n=n_m}^{n_{m+1}-1} |A_h(\overline{C}_h^m; \epsilon_{\boldsymbol{u}}^{n+1}, e_{\boldsymbol{u},h}^{n+1})| \leq 2A\Delta t \sum_{n=n_m}^{n_{m+1}-1} \|\epsilon_{\boldsymbol{u}}^{n+1}\|_h \|e_{\boldsymbol{u},h}^{n+1}\|_h \\
\leq & \frac{\alpha\Delta t}{7} \sum_{n=n_m}^{n_{m+1}-1} \|e_{\boldsymbol{u},h}^{n+1}\|_h^2 + \frac{7A^2\Delta t}{\alpha} \sum_{n=n_m}^{n_{m+1}-1} \|\epsilon_{\boldsymbol{u}}^{n+1}\|_h^2 \\
\leq & \frac{\alpha\Delta t}{7} \sum_{n=n_m}^{n_{m+1}-1} \|e_{\boldsymbol{u},h}^{n+1}\|_h^2 + \frac{7A^2R^2h^2\Delta t}{\alpha} \sum_{n=n_m}^{n_{m+1}-1} (|\boldsymbol{u}^{n+1}|_{2,s}^2 + |\boldsymbol{u}^{n+1}|_{2,d}^2).
\end{aligned} \tag{4.29}
$$

Similarly, from (3.15) and (4.2)

$$
\begin{aligned}
|S_5| \leq & 2\Delta t \sum_{n=n_m}^{n_{m+1}-1} |b_h(e_{\boldsymbol{u},h}^{n+1}, p^{n+1} - \Pi_h p^{n+1})| \leq 2\sqrt{L}\Delta t \sum_{n=n_m}^{n_{m+1}-1} \|e_{\boldsymbol{u},h}^{n+1}\|_h \|p^{n+1} - \Pi_h p^{n+1}\| \\
\leq & 2\sqrt{L}\Delta t P h \sum_{n=n_m}^{n_{m+1}-1} \|e_{\boldsymbol{u},h}^{n+1}\|_h (|p^{n+1}|_{1,s} + |p^{n+1}|_{1,d}) \\
\leq & \frac{\alpha\Delta t}{7} \sum_{n=n_m}^{n_{m+1}-1} \|e_{\boldsymbol{u},h}^{n+1}\|_h^2 + \frac{56LP^2h^2\Delta t}{\alpha} \sum_{n=n_m}^{n_{m+1}-1} (|p^{n+1}|_{1,s}^2 + |p^{n+1}|_{1,d}^2).
\end{aligned} \tag{4.30}
$$

In the same way as estimating T_3, follow the the assumption that $\boldsymbol{f}(c)$ is Lipschitz continuous, we obtain

$$
\begin{aligned}
|S_6| \leq & 2\Delta t \sum_{n=n_m}^{n_{m+1}-1} |F(c^{n+1}; e_{\boldsymbol{u},h}^{n+1}) - F(\overline{C}_h^m; e_{\boldsymbol{u},h}^{n+1})| \leq 2 f_L \Delta t \sum_{n=n_m}^{n_{m+1}-1} \|c^{n+1} - c_h^{n_m}\|_s \|e_{\boldsymbol{u},h}^{n+1}\|_h \\
\leq & \frac{\alpha\Delta t}{7} \sum_{n=n_m}^{n_{m+1}-1} \|e_{\boldsymbol{u},h}^{n+1}\|_h^2 + \frac{7f_L^2\Delta\tau}{\alpha} \|c^{n_m} - C_h^m\|_s^2 + \frac{7f_L^2((\Delta\tau)^2 + (\Delta t)^2)}{2\alpha} \int_{t_{n_m}}^{t_{n_{m+1}}} \|\partial_t c\|_s^2 dt.
\end{aligned} \tag{4.31}
$$

Using the proof of Lemma 5.3 in [37], we have

$$
\begin{aligned}
|S_7| \leq & 2\Delta t \sum_{n=n_m}^{n_{m+1}-1} \Big(2\mu_{\max} \sqrt{L(L+1)} C h |\boldsymbol{u}^{n+1}|_{2,s} \|e_{\boldsymbol{u},h}^{n+1}\|_h \\
& + \sqrt{(L+1)} C h (|p^{n+1}|_{1,s} + |p^{n+1}|_{1,d}) \|e_{\boldsymbol{u},h}^{n+1}\|_h + \sqrt{(L+1)} C h |p^{n+1}|_{1,d} \|e_{\boldsymbol{u},h}^{n+1}\|_h \Big) \\
\leq & \frac{\alpha\Delta t}{7} \sum_{n=n_m}^{n_{m+1}-1} \|e_{\boldsymbol{u},h}^{n+1}\|_h^2 + \sum_{n=n_m}^{n_{m+1}-1} \Big(\frac{84\mu_{\max}^2 L(L+1) C^2 h^2 \Delta t}{\alpha} |\boldsymbol{u}^{n+1}|_{2,s}^2 \\
& + \frac{21(L+1)C^2h^2\Delta t}{\alpha} |p^{n+1}|_{1,s}^2 + \frac{84(L+1)C^2h^2\Delta t}{\alpha} |p^{n+1}|_{1,d}^2 \Big),
\end{aligned} \tag{4.32}
$$

where C is a constant depending only on σ.

Taking the estimates of $S_1, S_2, \ldots, S_7$ back to (4.20) and summing over with $m = 0, 1, \ldots, l$, meanwhile, since $n_0 = 0$, we obtain

$$\begin{aligned}
&\|e_{\boldsymbol{u},h}^{n_{l+1}}\|_s^2 - \|e_{\boldsymbol{u},h}^0\|_s^2 + \alpha\Delta t \sum_{n=0}^{n_{l+1}-1} \|e_{\boldsymbol{u},h}^{n+1}\|_h^2 \\
\leq & \frac{7(\Delta t)^2}{3\alpha}\int_0^{T_1} \|\partial_t^2 \boldsymbol{u}\|_s^2 dt + \frac{7R^2h^2}{\alpha}\int_0^{T_1} |\partial_t \boldsymbol{u}|_{1,s}^2 dt \\
&+ \frac{21C\mu_L^2\Delta\tau}{\alpha}\sum_{m=0}^{l}(|c^{n_m} - C_h^m|_{1,s}^2 + \|c^{n_m} - C_h^m\|_s^2 + \frac{1}{k_{\min}^2}\|c^{n_m} - C_h^m\|_d^2) \\
&+ \frac{21C\mu_L^2((\Delta\tau)^2 + (\Delta t)^2)}{2\alpha}\int_0^{T_1}(|\partial_t c|_{1,s}^2 + \|\partial_t c\|_s^2 + \frac{1}{k_{\min}^2}\|\partial_t c\|_d^2)dt \\
&+ \frac{7A^2R^2h^2\Delta t}{\alpha}\sum_{n=0}^{n_{l+1}-1}(|\boldsymbol{u}^{n+1}|_{2,s}^2 + |\boldsymbol{u}^{n+1}|_{2,d}^2) + \frac{56LP^2h^2\Delta t}{\alpha}\sum_{n=0}^{n_{l+1}-1}(|p^{n+1}|_{1,s}^2 + |p^{n+1}|_{1,d}^2) \\
&+ \frac{7f_L^2\Delta\tau}{\alpha}\sum_{m=0}^{l}\|c^{n_m} - C_h^m\|_s^2 + \frac{7f_L^2((\Delta\tau)^2 + (\Delta t)^2)}{2\alpha}\int_0^{T_1}\|\partial_t c\|_s^2 dt \\
&+ \sum_{n=0}^{n_{l+1}-1}(\frac{84\mu_{\max}^2 L(L+1)C^2h^2\Delta t}{\alpha}|\boldsymbol{u}^{n+1}|_{2,s}^2 + \frac{21(L+1)C^2h^2\Delta t}{\alpha}|p^{n+1}|_{1,s}^2 \\
&+ \frac{84(L+1)C^2h^2\Delta t}{\alpha}|p^{n+1}|_{1,d}^2).
\end{aligned} \tag{4.33}$$

Using the property $\boldsymbol{u}_{h,s}^0 = \boldsymbol{r}_h\boldsymbol{u}_{s,0}$ and applying (3.17), we complete the proof. □

Now we consider the error estimate for concentration. At a certain time point $n_{m+1}, m = 0, 1, \ldots, M$, subtracting (3.10) from (2.29) and using (4.3) and (2.37), we have

$$\begin{aligned}
&(d_\tau e_{c,h}^{n_{m+1}}, z_h)_{\overline{\phi}} + (\overline{\boldsymbol{D}}(\boldsymbol{U}_h^m)\nabla e_{c,h}^{n_{m+1}}, \nabla z_h) \\
=&(d_\tau c^{n_{m+1}} - \partial_t c^{n_{m+1}}, z_h)_{\overline{\phi}} - (d_\tau \epsilon_c^{n_{m+1}}, z_h)_{\overline{\phi}} \\
&- ((\overline{\boldsymbol{D}}(\boldsymbol{u}^{n_{m+1}}) - \overline{\boldsymbol{D}}(\boldsymbol{U}_h^m))\nabla\Xi_h c^{n_{m+1}}, \nabla z_h) \\
&- \frac{1}{2}((\boldsymbol{u}^{n_{m+1}} - \boldsymbol{U}_h^m)\cdot\nabla\Xi_h c^{n_{m+1}}, z_h) - \frac{1}{2}(\boldsymbol{U}_h^m\cdot\nabla e_{c,h}^{n_{m+1}}, z_h) \\
&+ \frac{1}{2}((\boldsymbol{u}^{n_{m+1}} - \boldsymbol{U}_h^m)\Xi_h c^{n_{m+1}}, \nabla z_h) + \frac{1}{2}(\boldsymbol{U}_h^m e_{c,h}^{n_{m+1}}, \nabla z_h) \\
&- \frac{1}{2}((q^{I,n_{m+1}} + q^{P,n_{m+1}})(c^{n_{m+1}} - C_h^{m+1}), z_h)_d \\
&+ \frac{1}{2}((1 + q^{I,n_{m+1}} + q^{P,n_{m+1}})\epsilon_c^{n_{m+1}}, z_h)_d, \quad \forall z_h \in W_h.
\end{aligned} \tag{4.34}$$

Lemma 4.2. *Suppose that the analytical solution satisfies properties (4.9)–(4.11), if Δt and $\Delta\tau$ are sufficiently small, then there exists a positive constant $\hat{C}_3$ independent of h, Δt and $\Delta\tau$, and exists a positive constant $\hat{C}_4$ independent of h, Δt and $\Delta\tau$, and independent of physical parameters $\mu_{\max}$, $\mu_{\min}$, $k_{\min}$, $k_{\max}$, $D_{\min}$ and $\phi_{\max}$, such that for $0 \leq l \leq M-1$*

$$\|c^{n_{l+1}} - C_h^{l+1}\|^2 + D_{\min}\Delta\tau\sum_{m=0}^{l}\|\nabla(c^{n_{m+1}} - C_h^{m+1})\|^2$$

$$\leq \hat{C}_3 h^2 + \hat{C}_4\Big(\frac{1}{D_{\min}}(\Delta t)^2 + \phi_{\max}(\Delta\tau)^2\Big). \tag{4.35}$$

Proof. Taking $z_h = 2\Delta\tau e_{c,h}^{n_{m+1}}$ in (4.34), we have

$$\begin{aligned}
&2\Delta\tau(d_\tau e_{c,h}^{n_{m+1}}, e_{c,h}^{n_{m+1}})_{\overline{\phi}} + 2\Delta\tau(\overline{\boldsymbol{D}}(\boldsymbol{U}_h^m)\nabla e_{c,h}^{n_{m+1}}, \nabla e_{c,h}^{n_{m+1}})\\
=&2\Delta\tau(d_\tau c^{n_{m+1}} - \partial_t c^{n_{m+1}}, e_{c,h}^{n_{m+1}})_{\overline{\phi}} - 2\Delta\tau(d_\tau \epsilon_c^{n_{m+1}}, e_{c,h}^{n_{m+1}})_{\overline{\phi}}\\
&- 2\Delta\tau((\overline{\boldsymbol{D}}(\boldsymbol{u}^{n_{m+1}}) - \overline{\boldsymbol{D}}(\boldsymbol{U}_h^m))\nabla\Xi_h c^{n_{m+1}}, \nabla e_{c,h}^{n_{m+1}})\\
&- \Delta\tau((\boldsymbol{u}^{n_{m+1}} - \boldsymbol{U}_h^m)\cdot\nabla\Xi_h c^{n_{m+1}}, e_{c,h}^{n_{m+1}})\\
&+ \Delta\tau((\boldsymbol{u}^{n_{m+1}} - \boldsymbol{U}_h^m)\Xi_h c^{n_{m+1}}, \nabla e_{c,h}^{n_{m+1}})\\
&- \Delta\tau((q^{I,n_{m+1}} + q^{P,n_{m+1}})(c^{n_{m+1}} - C_h^{m+1}), e_{c,h}^{n_{m+1}})_d\\
&+ \Delta\tau((1 + q^{I,n_{m+1}} + q^{P,n_{m+1}})\epsilon_c^{n_{m+1}}, e_{c,h}^{n_{m+1}})_d\\
=&H_1 + H_2 + H_3 + H_4 + H_5 + H_6 + H_7,
\end{aligned} \tag{4.36}$$

using (2.24) and (4.19), we obtain

$$\|e_{c,h}^{n_{m+1}}\|_{\overline{\phi}}^2 - \|e_{c,h}^{n_m}\|_{\overline{\phi}}^2 + 2\Delta\tau D_{\min}\|\nabla e_{c,h}^{n_{m+1}}\|^2 \leq H_1 + H_2 + H_3 + H_4 + H_5 + H_6 + H_7. \tag{4.37}$$

Using Cauchy-Schwarz inequality, now we estimate $H_1, H_2, \ldots, H_7$ term by term.
Similarly as the estimates for S_1 and S_2, we have

$$\begin{aligned}
|H_1| =&|2\Delta\tau(d_\tau c^{n_{m+1}} - \partial_t c^{n_{m+1}}, e_{c,h}^{n_{m+1}})_{\overline{\phi}}|\\
\leq&\frac{\phi_{\max}\Delta\tau}{(\Delta\tau)^2}\int_\Omega\Big(\int_{\tau_m}^{\tau_{m+1}}(\partial_t^2 c(t))^2 dt\int_{\tau_m}^{\tau_{m+1}}(t-\tau_m)^2 dt\Big)dx + \Delta\tau\|e_{c,h}^{n_{m+1}}\|_{\overline{\phi}}^2\\
=&\frac{\phi_{\max}(\Delta\tau)^2}{3}\int_{\tau_m}^{\tau_{m+1}}\|\partial_t c\|^2 dt + \Delta\tau\|e_{c,h}^{n_{m+1}}\|_{\overline{\phi}}^2,
\end{aligned} \tag{4.38}$$

$$\begin{aligned}
|H_2| =&|2\Delta\tau(d_\tau \epsilon_c^{n_{m+1}}, e_{c,h}^{n_{m+1}})_{\overline{\phi}}|\\
\leq&\frac{\phi_{\max}\Delta\tau}{(\Delta\tau)^2}\int_\Omega\Big(\int_{\tau_m}^{\tau_{m+1}}(\partial_t\epsilon_c(t))^2 dt\int_{\tau_m}^{\tau_{m+1}} 1^2 dt\Big)dx + \Delta\tau\|e_{c,h}^{n_{m+1}}\|_{\overline{\phi}}^2\\
=&\phi_{\max}\int_{\tau_m}^{\tau_{m+1}}\|\partial_t\epsilon_c(t)\|^2 dt + \Delta\tau\|e_{c,h}^{n_{m+1}}\|_{\overline{\phi}}^2\\
\leq&\phi_{\max}h^2\int_{\tau_m}^{\tau_{m+1}}\|\partial_t c\|^2 dt + \Delta\tau\|e_{c,h}^{n_{m+1}}\|_{\overline{\phi}}^2.
\end{aligned} \tag{4.39}$$

Using (4.6) and (2.25), we have

$$\begin{aligned}
|H_3| =&|2\Delta\tau((\overline{D}(\boldsymbol{u}^{n_{m+1}}) - \overline{D}(\boldsymbol{U}_h^m))\nabla\Xi_h c^{n_{m+1}}, \nabla e_{c,h}^{n_{m+1}})|\\
\leq&2\Delta\tau C_c\|\overline{D}(\boldsymbol{u}^{n_{m+1}}) - \overline{D}(\boldsymbol{U}_h^m)\|\cdot\|\nabla e_{c,h}^{n_{m+1}}\|\\
\leq&\frac{2C_c^2\Delta\tau}{D_{\min}}(3d_l - 2d_t)\|\boldsymbol{u}^{n_{m+1}} - \boldsymbol{U}_h^m\|^2 + \frac{D_{\min}\Delta\tau}{2}\|\nabla e_{c,h}^{n_{m+1}}\|^2.
\end{aligned} \tag{4.40}$$

Here

$$\|\boldsymbol{u}^{n_{m+1}} - \boldsymbol{U}_h^m\|^2 = \frac{1}{r^2}\|r\boldsymbol{u}^{n_{m+1}} - \sum_{n=n_m}^{n_{m+1}-1} \boldsymbol{u}_h^{n+1}\|^2$$
$$\leq \frac{1}{r^2}\sum_{n=n_m}^{n_{m+1}-1} \|\boldsymbol{u}^{n_{m+1}} - \boldsymbol{u}_h^{n+1}\|^2$$
$$\leq \frac{1}{r^2}\sum_{n=n_m}^{n_{m+1}-1} \|\boldsymbol{u}^{n+1} - \boldsymbol{u}_h^{n+1}\|^2 + \frac{1}{r^2}\sum_{n=n_m}^{n_{m+1}-1} \|\boldsymbol{u}^{n_{m+1}} - \boldsymbol{u}^{n+1}\|^2. \tag{4.41}$$

From the discussion of (4.24), the second term of (4.41) can be estimated as follows

$$\frac{1}{r^2}\sum_{n=n_m}^{n_{m+1}-1} \|\boldsymbol{u}^{n_{m+1}} - \boldsymbol{u}^{n+1}\|^2 \leq \frac{1}{r}\sum_{n=n_m}^{n_{m+1}-1} \|\boldsymbol{u}^{n+1} - \boldsymbol{u}^{n}\|^2. \tag{4.42}$$

Taking (4.41) and (4.42) back to (4.40), we get the estimate of H_3

$$|H_3| \leq \frac{2C_c^2\Delta\tau}{D_{\min}r}(3d_l - 2d_t)\sum_{n=n_m}^{n_{m+1}-1} \|\boldsymbol{u}^{n+1} - \boldsymbol{u}^{n}\|^2 + \frac{2C_c^2\Delta\tau}{D_{\min}r^2}(3d_l - 2d_t)\sum_{n=n_m}^{n_{m+1}-1} \|\boldsymbol{u}^{n+1} - \boldsymbol{u}_h^{n+1}\|^2$$
$$+ \frac{D_{\min}\Delta\tau}{2}\|\nabla e_{c,h}^{n_{m+1}}\|^2$$
$$\leq \frac{2C_c^2(\Delta t)^2}{D_{\min}}(3d_l - 2d_t)\int_{t_{n_m}}^{t_{n_{m+1}}} \|\partial_t\boldsymbol{u}\|^2 dt + \frac{2C_c^2\Delta t}{D_{\min}r}(3d_l - 2d_t)\sum_{n=n_m}^{n_{m+1}-1} \|\boldsymbol{u}^{n+1} - \boldsymbol{u}_h^{n+1}\|^2$$
$$+ \frac{D_{\min}\Delta\tau}{2}\|\nabla e_{c,h}^{n_{m+1}}\|^2. \tag{4.43}$$

Similarly, H_4 and H_5 can also be estimated as follows

$$|H_4| = |\Delta\tau((\boldsymbol{u}^{n_{m+1}} - \boldsymbol{U}_h^m)\cdot\nabla\Xi_h c^{n_{m+1}}, e_{c,h}^{n_{m+1}})|$$
$$\leq \Delta\tau C_c\|\boldsymbol{u}^{n_{m+1}} - \boldsymbol{U}_h^m\|\cdot\|e_{c,h}^{n_{m+1}}\|$$
$$\leq \frac{C_c^2\Delta\tau}{4}\|\boldsymbol{u}^{n_{m+1}} - \boldsymbol{U}_h^m\|^2 + \Delta\tau\|e_{c,h}^{n_{m+1}}\|^2$$
$$\leq \frac{C_c^2(\Delta t)^2}{4}\int_{t_{n_m}}^{t_{n_{m+1}}} \|\partial_t\boldsymbol{u}\|^2 dt + \frac{C_c^2\Delta t}{4r}\sum_{n=n_m}^{n_{m+1}-1} \|\boldsymbol{u}^{n+1} - \boldsymbol{u}_h^{n+1}\|^2 + \Delta\tau\|e_{c,h}^{n_{m+1}}\|^2, \tag{4.44}$$

$$|H_5| = |\Delta\tau((\boldsymbol{u}^{n_{m+1}} - \boldsymbol{U}_h^m)\Xi_h c^{n_{m+1}}, \nabla e_{c,h}^{n_{m+1}})|$$
$$\leq \Delta\tau C_c\|\boldsymbol{u}^{n_{m+1}} - \boldsymbol{U}_h^m\|\cdot\|\nabla e_{c,h}^{n_{m+1}}\|$$
$$\leq \frac{C_c^2\Delta\tau}{2D_{\min}}\|\boldsymbol{u}^{n_{m+1}} - \boldsymbol{U}_h^m\|^2 + \frac{D_{\min}\Delta\tau}{2}\|\nabla e_{c,h}^{n_{m+1}}\|^2$$
$$\leq \frac{C_c^2(\Delta t)^2}{2D_{\min}}\int_{t_{n_m}}^{t_{n_{m+1}}} \|\partial_t\boldsymbol{u}\|^2 dt + \frac{C_c^2\Delta t}{2D_{\min}r}\sum_{i=n_m}^{n_{m+1}-1} \|\boldsymbol{u}^{n+1} - \boldsymbol{u}_h^{n+1}\|^2 + \frac{D_{\min}\Delta\tau}{2}\|\nabla e_{c,h}^{n_{m+1}}\|^2. \tag{4.45}$$

The last two terms H_6 and H_7 can be estimated directly

$$\begin{aligned}|H_6| =&|\Delta\tau((q^{I,n_{m+1}} + q^{P,n_{m+1}})(c^{n_{m+1}} - C_h^m), e_{c,h}^{n_{m+1}})_d|\\ \le&(q_{\max}^I + q_{\max}^P)\Delta\tau\|c^{n_{m+1}} - C_h^m\|_d \cdot \|e_{c,h}^{n_{m+1}}\|_d\\ \le&(q_{\max}^I + q_{\max}^P)\Delta\tau(\frac{1}{2}\|c^{n_{m+1}} - c_h^{n_{m+1}}\|_d^2 + \frac{1}{2}\|e_{c,h}^{n_{m+1}}\|_d^2)\\ \le&\frac{1}{2}(q_{\max}^I + q_{\max}^P)\Delta\tau\|\epsilon_c^{n_{m+1}}\|^2 + (q_{\max}^I + q_{\max}^P)\Delta\tau\|e_{c,h}^{n_{m+1}}\|^2,\end{aligned} \tag{4.46}$$

$$\begin{aligned}|H_7| =&|\Delta\tau((1 + q^{I,n_{m+1}} + q^{P,n_{m+1}})\epsilon_c^{n_{m+1}}, e_{c,h}^{n_{m+1}})_d|\\ \le&(1 + q_{\max}^I + q_{\max}^P)\Delta\tau\|\epsilon_c^{n_{m+1}}\|_d \cdot \|e_{c,h}^{n_{m+1}}\|_d\\ \le&\frac{1}{2}(1 + q_{\max}^I + q_{\max}^P)\Delta\tau\|\epsilon_c^{n_{m+1}}\|^2 + \frac{1}{2}(1 + q_{\max}^I + q_{\max}^P)\Delta\tau\|e_{c,h}^{n_{m+1}}\|^2.\end{aligned} \tag{4.47}$$

Collecting each estimate above and summing over with $m = 0, 1, \ldots, l$, due to the fact that $e_{c,h}^{n_0} = 0$ and $(\cdot,\cdot)_{\overline{\phi}}$ is an equivalent scalar product on $L^2(\Omega)$, we have

$$\begin{aligned}\|e_{c,h}^{n_{l+1}}\|^2 + D_{\min}\Delta\tau\sum_{m=0}^{l}\|\nabla e_{c,h}^{n_{m+1}}\|^2 \le&\tilde{C}_1\Big(h^2\int_0^{T_1}\|\partial_t c\|^2 dt + \Delta\tau\sum_{m=0}^{l}\|e_{c,h}^{n_{m+1}}\|^2\\ &+ \Delta t\sum_{n=0}^{n_{l+1}-1}\|\boldsymbol{u}^{n+1} - \boldsymbol{u}_h^{n+1}\|^2 + \Delta\tau\sum_{m=0}^{l}\|\epsilon_c^{n_{m+1}}\|^2\Big)\\ &+ \hat{C}_4\Big(\frac{1}{D_{\min}}(\Delta t)^2 + \phi_{\max}(\Delta\tau)^2\Big).\end{aligned} \tag{4.48}$$

If Δt and $\Delta\tau$ are sufficiently small, applying the discrete Gronwalll inequality and using (4.17) in Lemma 4.1, we can obtain

$$\|e_{c,h}^{n_{l+1}}\|^2 + D_{\min}\Delta\tau\sum_{m=0}^{l}\|\nabla e_{c,h}^{n_{m+1}}\|^2 \le\tilde{C}_2 h^2 + \hat{C}_4\Big(\frac{1}{D_{\min}}(\Delta t)^2 + \phi_{\max}(\Delta\tau)^2\Big). \tag{4.49}$$

Here positive constants $\tilde{C}_1$ and $\tilde{C}_2$ are independent of h, Δt and $\Delta\tau$. Combining with the estimate for $c - \Xi_h c$ in (4.4) and the setting $C_h^m = c_h^{n_m}$, we get (4.35). □

Combining the above two lemmas, we give the error estimate conclusion solely in terms of Δt under appropriate ratio r, which determine time steps for each equation.

Theorem 4.2. *Suppose that the analytical solution satisfies properties (4.9)–(4.11). Let*

$$r = \hat{C}_5\Big(\frac{k_{\max}k_{\min}^2 D_{\min} + k_{\max}D_{\min} + \mu_{\min}k_{\min}^2}{k_{\max}k_{\min}^2 D_{\min} + k_{\max}D_{\min} + \phi_{\max}\mu_{\min}k_{\min}^2 D_{\min}}\Big)^{\frac{1}{2}}, \tag{4.50}$$

where the positive constant $\hat{C}_5$ is independent of physical parameters $\mu_{\max}$, $\mu_{\min}$, $k_{\min}$, $k_{\max}$, $D_{\min}$ and $\phi_{\max}$. If Δt is sufficiently small, then there exists a positive constant $\hat{C}_6$ independent of h and Δt, and *exists a positive constant $\hat{C}_7$ independent of h and Δt, and independent of physical parameters $\mu_{\max}$, $\mu_{\min}$, $k_{\min}$, $k_{\max}$, $D_{\min}$ and $\phi_{\max}$, such that for* $0 \le l \le M-1$

$$\begin{aligned}
&\|\boldsymbol{u}^{n_{l+1}} - \boldsymbol{u}_h^{n_{l+1}}\|_s^2 + \alpha\Delta t \sum_{n=0}^{n_{l+1}-1} \|\boldsymbol{u}^{n+1} - \boldsymbol{u}_h^{n+1}\|_h^2 \\
&+ \|c^{n_{l+1}} - C_h^{l+1}\|^2 + D_{\min}\Delta\tau \sum_{m=0}^{l} \|\nabla(c^{n_{m+1}} - C_h^{m+1})\|^2 \\
\le& \hat{C}_6 h^2 + \hat{C}_7\Big(\frac{k_{\max}}{\mu_{\min}} + \frac{k_{\max}}{\mu_{\min}k_{\min}^2} + \frac{1}{D_{\min}}\Big)(\Delta t)^2. \qquad (4.51)
\end{aligned}$$

Proof. From Lemmas 4.1 and 4.2, $\alpha \propto \dfrac{\mu_{\min}}{k_{\max}}$ in Lemma 3.2 and $\Delta\tau = r \cdot \Delta t$, we have

$$\begin{aligned}
&\|\boldsymbol{u}^{n_{l+1}} - \boldsymbol{u}_h^{n_{l+1}}\|_s^2 + \alpha\Delta t \sum_{n=0}^{n_{l+1}-1} \|\boldsymbol{u}^{n+1} - \boldsymbol{u}_h^{n+1}\|_h^2 \\
&+ \|c^{n_{l+1}} - C_h^{l+1}\|^2 + D_{\min}\Delta\tau \sum_{m=0}^{l} \|\nabla(c^{n_{m+1}} - C_h^{m+1})\|^2 \\
\le& \hat{C}_6 h^2 + \hat{C}_8\Big(\big(\frac{k_{\max}}{\mu_{\min}} + \frac{k_{\max}}{\mu_{\min}k_{\min}^2} + \frac{1}{D_{\min}}\big) + \big(\frac{k_{\max}}{\mu_{\min}} + \frac{k_{\max}}{\mu_{\min}k_{\min}^2} + \phi_{\max}\big)r^2\Big)(\Delta t)^2,
\end{aligned}$$

where $\hat{C}_8 = \max\{\hat{C}_2, \hat{C}_4\}$. We derive the estimate (4.51) by taking $\hat{C}_7 = \hat{C}_8(1 + (\hat{C}_5)^2)$. □

5. Numerical experiments

In this section we give some numerical experiments to demonstrate the error estimates results obtained in the previous section. For simplicity, take the unit square domain $\Omega = [0,1] \times [0,1]$, and choose $\Omega_s = [0,1/2] \times [0,1]$ and $\Omega_d = [1/2,1] \times [0,1]$ with the interface $\Gamma_I = \{1/2\} \times (0,1)$. The time interval is $J = [0,2]$. Unless specified otherwise, for all the numerical experiments the values of the parameters are assigned as $\phi = 0.3,\ \gamma = d = q^I = 1$, $K = \frac{1}{2}\boldsymbol{I}$, and

$$\boldsymbol{D}(\boldsymbol{u}) = \begin{bmatrix} 1 & 0 \\ 0 & 1 + u_2^2 \end{bmatrix},$$

which can be obtained that $D_{min} = 1$. $\mathscr{T}_h$ is taken as a uniform grid. The upper and lower bounds of μ in (2.20) are $\mu(1) = 1.2$ and $\mu(0) = 0.1$. Since it is difficult to construct the exact solutions that satisfy the entire coupled Stokes and Darcy flows with mass transfer (2.1)–(2.16), especially the interface conditions. To solve this, we generalize the interface conditions (2.8), (2.9) and (2.11) to include nonhomogeneous terms.

$$\begin{aligned}
&p_s - \boldsymbol{n}_s \cdot 2\mu(c_s)\boldsymbol{S}(\boldsymbol{u}_s) \cdot \boldsymbol{n}_s = p_d + \eta_1, \\
&2\boldsymbol{n}_s \cdot \mu(c_s)\boldsymbol{S}(\boldsymbol{u}_s) \cdot \boldsymbol{\tau}_I + \mu(c_s)\gamma\boldsymbol{u}_s \cdot \boldsymbol{\tau}_I = \eta_2, \\
&d\nabla c_s \cdot \boldsymbol{n}_s + \boldsymbol{D}(\boldsymbol{u}_d)\nabla c_d \cdot \boldsymbol{n}_d = \eta_3,
\end{aligned}$$

where η_1, η_2 and η_3 are given functions on Γ_I according to the analytical solutions. The variational form for this modified system will only include two additional terms $-\langle \eta_1, \boldsymbol{v}_s \cdot \boldsymbol{n}_s \rangle_{\Gamma_I} + \langle \eta_2, \boldsymbol{v}_s \cdot \boldsymbol{\tau}_I \rangle_{\Gamma_I}$ to the right-hand side of (2.27), and one additional term $-\langle \eta_3, z \rangle_{\Gamma_I}$ to the right-hand side of (2.29). All the right-hand terms and boundary conditions are selected according to the analytical solution.

Notation wise, We define the following symbols to represent the computational errors.

$$
\begin{aligned}
&||e_s^{\boldsymbol{u}}||_{l^\infty(L^2)} = \max_n ||\boldsymbol{u}^n - \boldsymbol{u}_h^n||_s, \quad ||e_d^{\boldsymbol{u}}||_{l^\infty(L^2)} = \max_n ||\boldsymbol{u}^n - \boldsymbol{u}_h^n||_d, \\
&||e^{\boldsymbol{u}}||_{l^\infty(L^2)} = \max_n \left(||\boldsymbol{u}^n - \boldsymbol{u}_h^n||_s^2 + ||\boldsymbol{u}^n - \boldsymbol{u}_h^n||_d^2 \right)^{1/2}, \quad |e_s^{\boldsymbol{u}}|_{l^\infty(H^1)} = \max_n |\boldsymbol{u}^n - \boldsymbol{u}_h^n|_{1,s} \\
&||e_s^{p}||_{l^\infty(L^2)} = \max_n ||p^n - p_h^n||_s, \quad ||e_d^{p}||_{l^\infty(L^2)} = \max_n ||p^n - p_h^n||_d, \\
&||e^{p}||_{l^\infty(L^2)} = \max_n \left(||p^n - p_h^n||_s^2 + ||p^n - p_h^n||_d^2 \right)^{1/2}, \\
&||e^{c}||_{l^\infty(L^2)} = \max_m ||c^{n_m} - C_h^m||.
\end{aligned} \tag{5.1}
$$

With these notations, we compute the convergence rate of the approximate solutions by

$$
rate = \frac{\log(||E^{h_1}||/||E^{h_2}||)}{\log(h_1/h_2)}, \tag{5.2}
$$

with meshsizes h_1 and h_2. $E^{h_i}, i = 1, 2$ are any of the errors described in (5.1).

We will use two different numerical examples to verify the convergence rates of the multiple time step discrete finite element schemes (3.8)–(3.10). In each example we also compare the errors, convergence rates and CPU calculation time for concentration (unit:second) of the single time step discrete finite element scheme (which means $r = 1$, $M = N$, $\Delta t = \Delta\tau$) and the multiple time step discrete finite element scheme.

We list and plot all the errors in (5.1) and calculate the corresponding convergence rates for h, which is set to $2^{-m}, m = 2, 3, 4, 5$. The number of time steps is $N = 100$, and r in the multiple time step discrete finite element scheme is set to be $r = 20$. To make this setting valid, we take $\hat{C}_5 \approx 19.73$, so that $M = 5$.

Example 5.1. *In this example, the analytical velocity, pressure and concentration in Stokes domain and Darcy domain are listed as follows*

$$
\begin{cases}
\boldsymbol{u}_s = (\sin(y^2 + 6x + t), \cos(4x^2 y) e^t)^T, & p_s = 2(y-1)\cos^2 x e^t, \\
\boldsymbol{u}_d = (\sin(y^2 + 6x + t), \sin(2x)\cos(3y) t^2)^T, & p_d = y \cos y^2 + 4x - \dfrac{5}{2} + t, \\
c_s = c_d = x(1-x)y(1-y)e^{-t}.
\end{cases}
$$

The numerical results, convergence rates and CPU calculation time of Example 5.1 are listed in Tables 1 and 2. The convergence rates are plotted with respect of nodes on each direction in Figure 3. The numerical velocity quiver, numerical pressure distribution and numerical concentration distribution of the multiple time step discrete finite element scheme with $h = 1/32$ are plotted in Figures 4 and 5.

Table 1. The convergence performance and CPU time of Example 5.1 by using single time step discrete finite element scheme ($r = 1$).

h	$\|\|e_s^{\boldsymbol{u}}\|\|_{l^\infty(L^2)}$	$\|\|e_d^{\boldsymbol{u}}\|\|_{l^\infty(L^2)}$	$\|\|e^{\boldsymbol{u}}\|\|_{l^\infty(L^2)}$	$\|e_s^{\boldsymbol{u}}\|_{l^\infty(H^1)}$	$\|\|e^c\|\|_{l^\infty(L^2)}$
1/4	$4.09e-2$	$1.17e-1$	$1.25e-1$	$1.03e+0$	$4.35e-3$
1/8	$1.39e-2$	$5.81e-2$	$5.97e-2$	$5.34e-1$	$1.15e-3$
1/16	$3.83e-3$	$2.66e-2$	$2.68e-2$	$2.71e-1$	$2.88e-4$
1/32	$9.90e-4$	$1.11e-2$	$1.11e-2$	$1.36e-1$	$7.24e-5$
rate	1.95	1.26	1.27	0.99	1.99
h	$\|\|e_s^p\|\|_{l^\infty(L^2)}$	$\|\|e_d^p\|\|_{l^\infty(L^2)}$	$\|\|e^p\|\|_{l^\infty(L^2)}$	CPU time (s)	
1/4	$1.39e-1$	$1.61e-1$	$2.13e-1$	0.07	
1/8	$8.15e-2$	$8.67e-2$	$1.19e-1$	0.88	
1/16	$4.28e-2$	$4.52e-2$	$6.23e-2$	36.77	
1/32	$2.18e-2$	$2.31e-2$	$3.17e-2$	1733.81	
rate	0.97	0.97	0.97	-	

Table 2. The convergence performance and CPU time of Example 5.1 by using multiple time step discrete finite element scheme ($r = 20$).

h	$\|\|e_s^{\boldsymbol{u}}\|\|_{l^\infty(L^2)}$	$\|\|e_d^{\boldsymbol{u}}\|\|_{l^\infty(L^2)}$	$\|\|e^{\boldsymbol{u}}\|\|_{l^\infty(L^2)}$	$\|e_s^{\boldsymbol{u}}\|_{l^\infty(H^1)}$	$\|\|e^c\|\|_{l^\infty(L^2)}$
1/4	$4.30e-2$	$1.17e-1$	$1.25e-1$	$1.03e+0$	$3.89e-3$
1/8	$1.42e-2$	$5.81e-2$	$5.98e-2$	$5.35e-1$	$1.03e-3$
1/16	$3.86e-3$	$2.66e-2$	$2.69e-2$	$2.72e-1$	$2.60e-4$
1/32	$9.95e-4$	$1.13e-2$	$1.13e-2$	$1.36e-1$	$6.55e-5$
rate	1.96	1.24	1.25	1.00	1.99
h	$\|\|e_s^p\|\|_{l^\infty(L^2)}$	$\|\|e_d^p\|\|_{l^\infty(L^2)}$	$\|\|e^p\|\|_{l^\infty(L^2)}$	CPU time (s)	
1/4	$1.40e-1$	$1.61e-1$	$2.14e-1$	0.005	
1/8	$8.17e-2$	$8.68e-2$	$1.19e-1$	0.046	
1/16	$4.28e-2$	$4.53e-2$	$6.23e-2$	1.83	
1/32	$2.19e-2$	$2.31e-2$	$3.18e-2$	86.82	
rate	0.97	0.97	0.97	-	

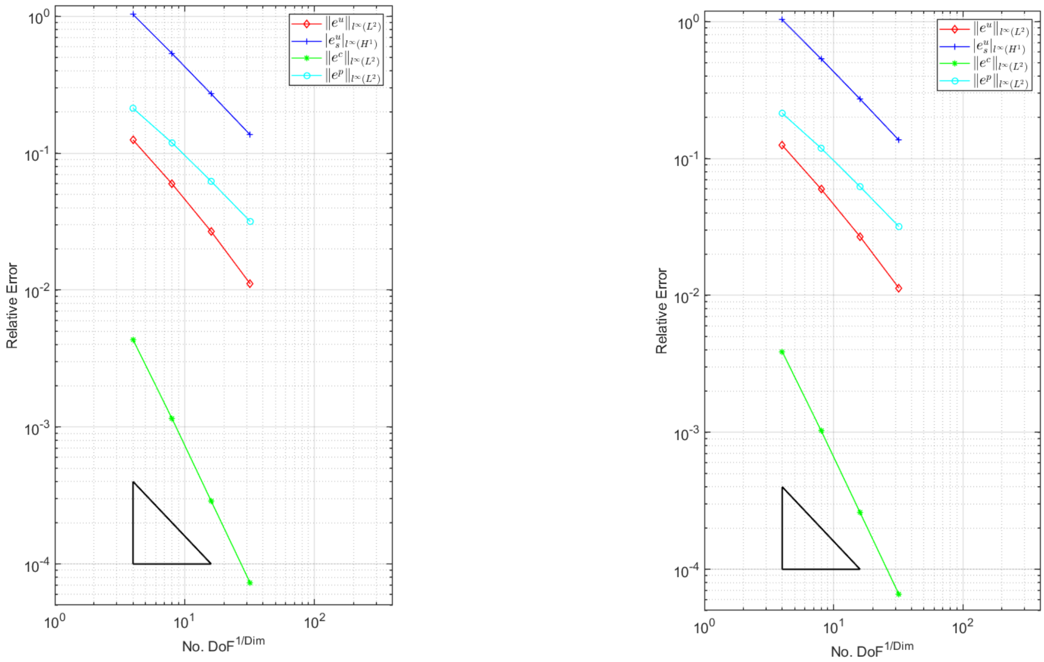

$r = 1$ $\qquad$ $r = 20$

Figure 3. Convergence rates of Example 5.1. The tangent of the triangle is 1.

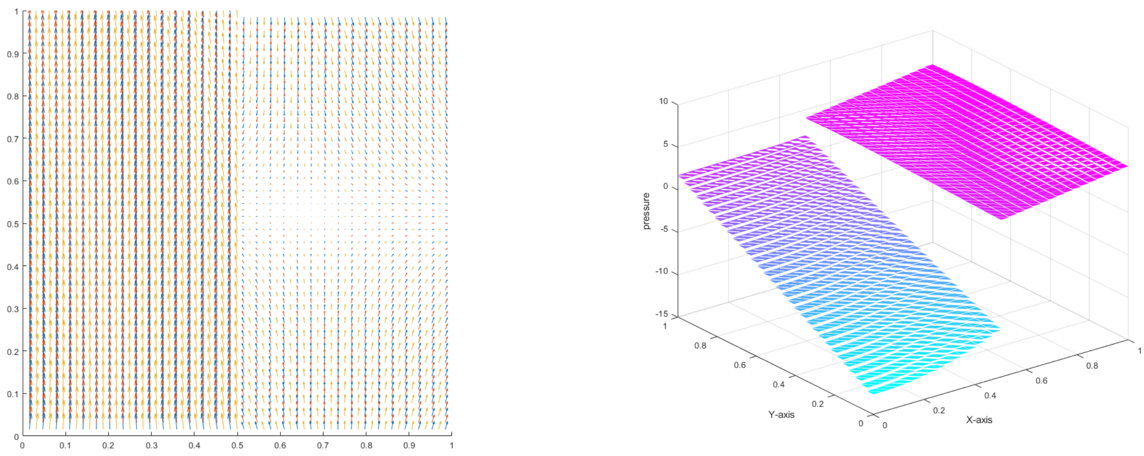

Figure 4. Numerical velocity quiver (left figure) and numerical pressure distribution (right figure) of Example 5.1 at time 2.0.

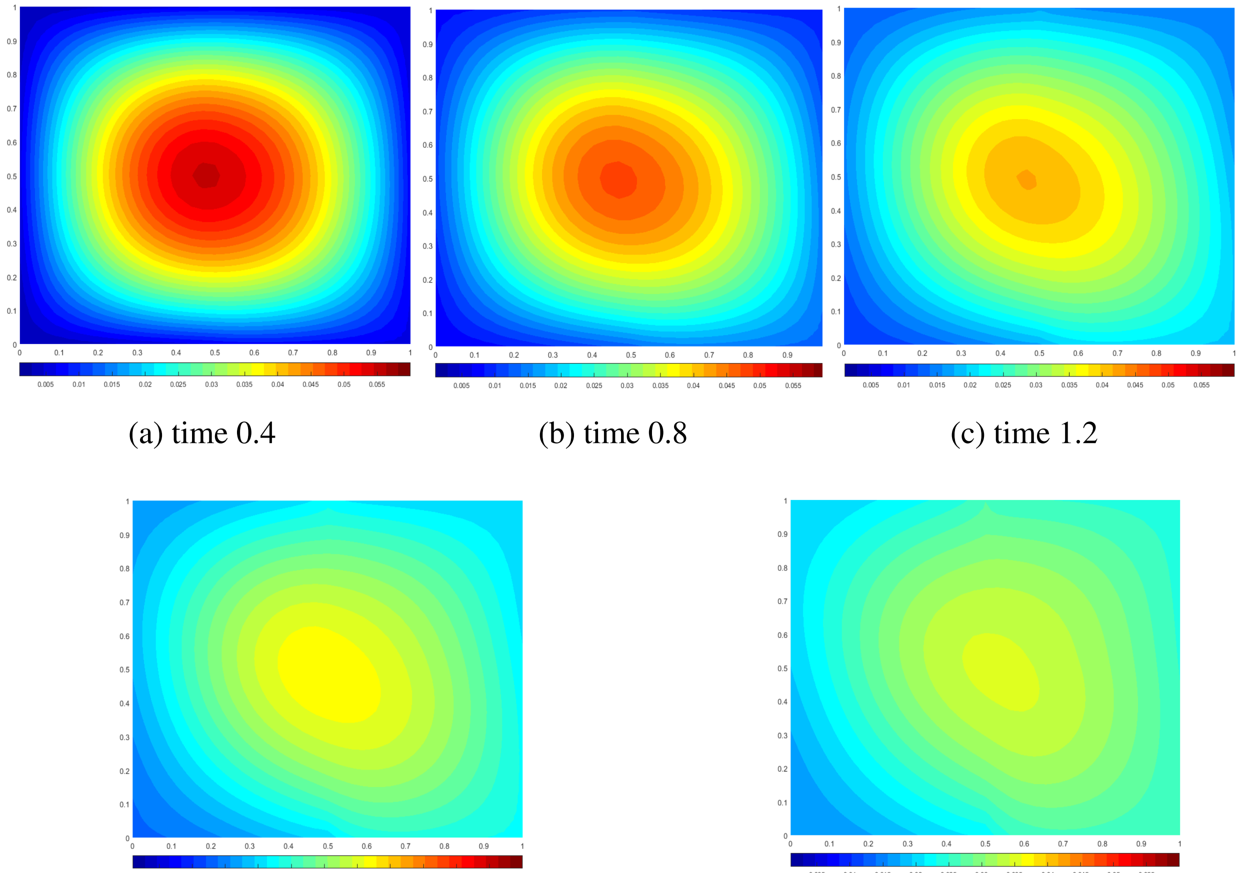

(a) time 0.4 (b) time 0.8 (c) time 1.2

(d) time 1.6 (e) time 2.0

Figure 5. Numerical concentration of Example 5.1.

Example 5.2. *In this example, the analytical velocity, pressure and concentration in Stokes domain and Darcy domain are listed as follows*

$$\begin{cases} \boldsymbol{u}_s = (e^{-(x+2y+t)}, e^{xy}\sin(t))^T, & p_s = 12x^2e^y\sin(2t), \\ \boldsymbol{u}_d = (e^{-(x+2y+t)}, 2e^{-(x+2y+2t)})^T, & p_d = (16xy^3-2)\cos(2t), \\ c_s = c_d = \sin(\pi x)\sin(\pi y)e^{-t}. \end{cases}$$

The numerical results, convergence rates and CPU calculation time of Example 5.2 are listed in Tables 3 and 4. The convergence rates are plotted with respect of nodes on each direction in Figure 6. The numerical velocity quiver, numerical pressure distribution and numerical concentration distribution of the multiple time step discrete finite element scheme with $h = 1/32$ are plotted in Figures 7 and 8.

Table 3. The convergence performance and CPU time of Example 5.2 by using single time step discrete finite element scheme ($r = 1$).

h	$\|\|e_s^{\boldsymbol{u}}\|\|_{l^\infty(L^2)}$	$\|\|e_d^{\boldsymbol{u}}\|\|_{l^\infty(L^2)}$	$\|\|e^{\boldsymbol{u}}\|\|_{l^\infty(L^2)}$	$\|e_s^{\boldsymbol{u}}\|_{l^\infty(H^1)}$	$\|\|e^c\|\|_{l^\infty(L^2)}$
1/4	$8.30e-3$	$2.37e-2$	$6.40e-2$	$1.32e-1$	$3.66e-2$
1/8	$1.93e-3$	$5.93e-3$	$1.62e-2$	$6.15e-2$	$1.34e-2$
1/16	$5.01e-4$	$1.78e-3$	$3.98e-3$	$2.30e-2$	$4.56e-3$
1/32	$1.56e-4$	$8.74e-4$	$1.57e-3$	$8.62e-3$	$1.39e-3$
rate	1.68	1.03	1.34	1.42	1.71
h	$\|\|e_s^p\|\|_{l^\infty(L^2)}$	$\|\|e_d^p\|\|_{l^\infty(L^2)}$	$\|\|e^p\|\|_{l^\infty(L^2)}$	CPU time (s)	
1/4	$1.96e-1$	$4.57e-1$	$5.81e-1$	0.09	
1/8	$1.17e-1$	$2.59e-1$	$2.93e-1$	0.92	
1/16	$6.03e-2$	$1.34e-1$	$1.47e-1$	38.58	
1/32	$3.02e-2$	$6.73e-2$	$7.38e-2$	1842.36	
rate	1.00	0.99	0.99	-	

Table 4. The convergence performance and CPU time of Example 5.2 by using multiple time step discrete finite element scheme ($r = 20$).

h	$\|\|e_s^{\boldsymbol{u}}\|\|_{l^\infty(L^2)}$	$\|\|e_d^{\boldsymbol{u}}\|\|_{l^\infty(L^2)}$	$\|\|e^{\boldsymbol{u}}\|\|_{l^\infty(L^2)}$	$\|e_s^{\boldsymbol{u}}\|_{l^\infty(H^1)}$	$\|\|e^c\|\|_{l^\infty(L^2)}$
1/4	$8.30e-3$	$2.38e-2$	$6.42e-2$	$1.32e-1$	$4.16e-2$
1/8	$1.93e-3$	$6.11e-3$	$1.61e-2$	$6.15e-2$	$1.54e-2$
1/16	$5.03e-4$	$1.80e-3$	$3.98e-3$	$2.30e-2$	$4.87e-3$
1/32	$1.59e-4$	$8.75e-4$	$1.59e-3$	$8.63e-3$	$1.52e-3$
rate	1.66	1.04	1.32	1.41	1.68
h	$\|\|e_s^p\|\|_{l^\infty(L^2)}$	$\|\|e_d^p\|\|_{l^\infty(L^2)}$	$\|\|e^p\|\|_{l^\infty(L^2)}$	CPU time (s)	
1/4	$1.96e-1$	$4.57e-1$	$5.81e-1$	0.008	
1/8	$1.17e-1$	$2.59e-1$	$2.93e-1$	0.055	
1/16	$6.03e-2$	$1.34e-1$	$1.47e-1$	2.01	
1/32	$3.02e-2$	$6.73e-2$	$7.38e-2$	99.11	
rate	1.00	0.99	0.99	-	

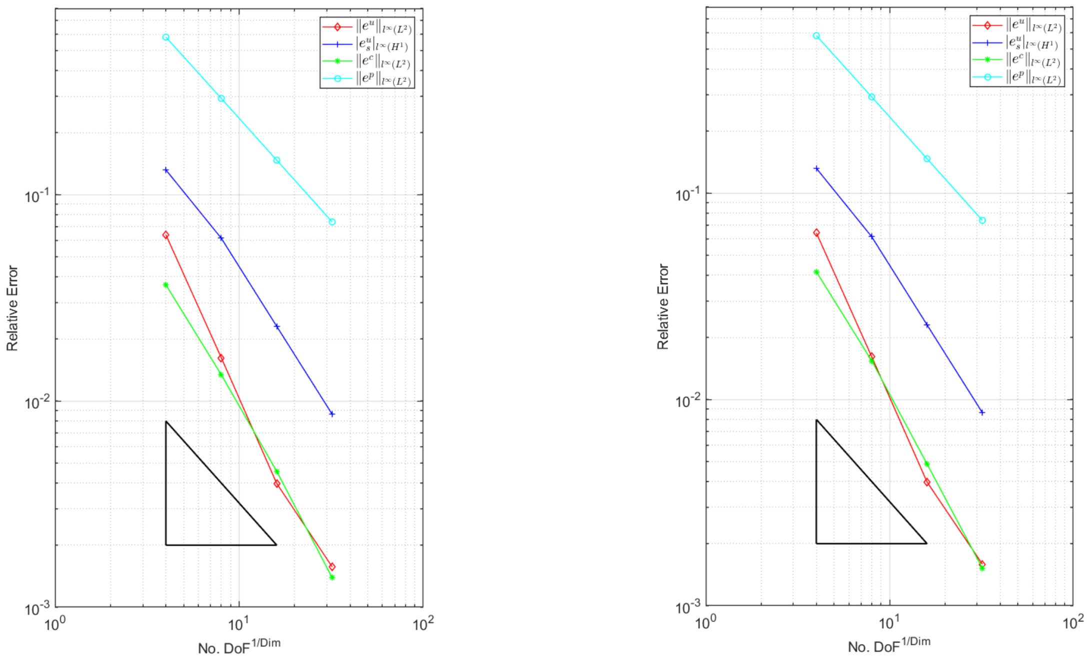

$r = 1$ $r = 20$

Figure 6. Convergence rates of Example 5.2. The tangent of the triangle is 1.

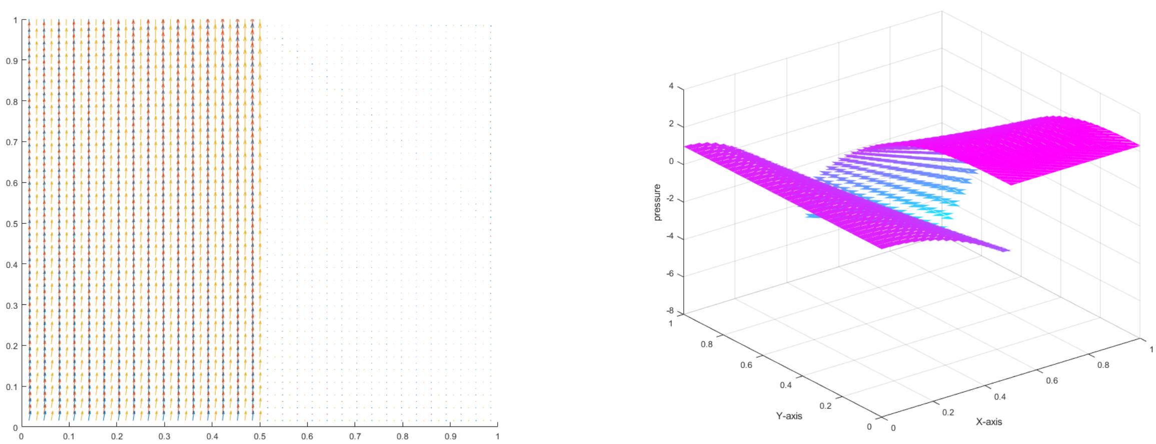

Figure 7. Numerical velocity quiver (left figure) and numerical pressure distribution (right figure) of Example 5.2 at time 2.0.

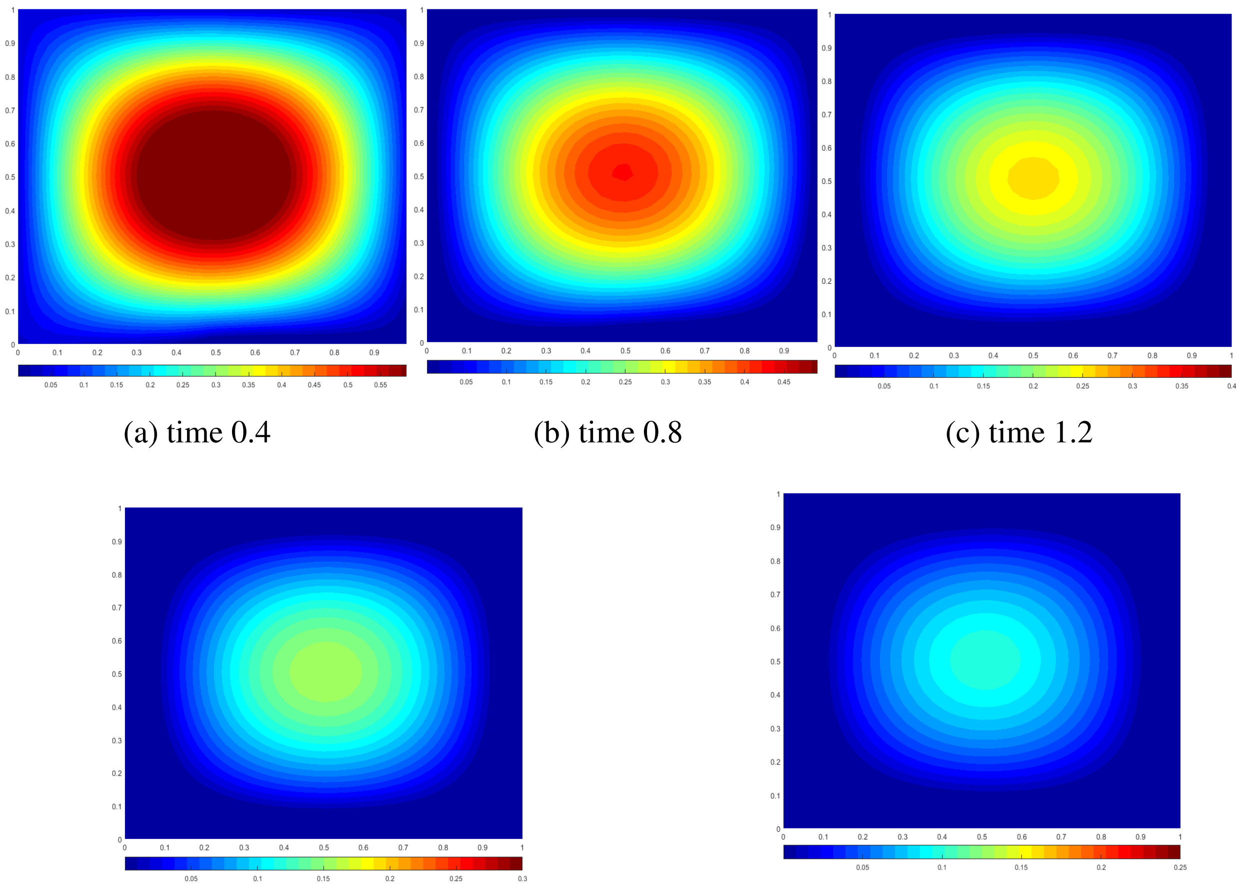

(a) time 0.4 (b) time 0.8 (c) time 1.2

(d) time 1.6 (e) time 2.0

Figure 8. Numerical concentration of Example 5.2.

From Tables 1–4, Figures 3 and 4, we find that the numerical results are consistent with the theoretical analysis. The convergence rates for the pressure and velocity on Ω in $l^\infty(L^2)$ norm and the velocity on Ω_s in $l^\infty(H^1)$ norm are first-order, and the convergence rate for the velocity on Ω_s in $l^\infty(L^2)$ norm and the concentration on Ω in $l^\infty(L^2)$ norm are at least first-order. All the convergence rates are optimal. About the superconvergence for the velocity on Ω_s in $l^\infty(L^2)$ norm and the concentration on Ω in $l^\infty(L^2)$ norm, we have no approach to give the corresponding analysis temporarily, the theoretical investigation of the phenomena will be our future work.

From the comparison of Tables 1 and 2, Tables 3 and 4, we find that, the errors are similar in every discretization parameter, and the convergence rates are the same, but the multiple time step discrete finite element scheme costs less CPU time. And from Figures 4 and 5 and Figures 7 and 8, we can see that, it can clearly reflect the modification of velocity, pressure and concentration by using multiple time step discrete finite element scheme with fewer time steps for concentration. The comparison verify that the multiple time step method is useful to increase computational efficiency.

6. Conclusions

This article presents a stabilized finite element algorithm with different time steps on different physical variables for the coupled Stokes-Darcy flows system with the solution transport (2.1)–(2.16). We use nonconforming piecewise linear Crouzeix-Raviart element and piecewise constant to approximate velocity and pressure in the coupled Stokes-Darcy flows system, and use conforming piecewise linear finite element to approximate concentration in the transport system. The time derivatives are discretized with different step sizes in these two systems. The existence and uniqueness of the approximate solution are proved unconditionally satisfied. The order of convergence and error estimates are given, which also provide a guidance on the ratio of time step sizes with respect to the ratio of the physical parameters. We present two numerical examples to verify that the numerical results are in agreement with the theoretical analysis. The results obtained through our numerical examples indicate that we can obtain optimal error estimation order by using the multiple time step discrete finite element scheme provided in this article and reduce computation, effectively improve computational efficiency.

Use of AI tools declaration

The authors declare they have not used Artificial Intelligence (AI) tools in the creation of this article.

Acknowledgments

The author would like to thank the referees for the helpful suggestions.

The work is supported by the National Natural Science Foundation of China No.12001308 and the Natural Science Foundation of Shandong Province No.ZR2021QF040.

Conflict of interest

The authors declare no conflicts of interest in this paper.

References

1. C. Bernardi, F. Hecht, F. Z. Nouri, A new finite-element discretization of the Stokes problem coupled with the Darcy equations, *IMA J. Numer. Anal.*, **30** (2010), 61–93. https://doi.org/10.1093/imanum/drn054
2. Y. Boubendir, S. Tlupova, Domain decomposition methods for solving Stokes-Darcy problems with boundary integrals, *SIAM J. Sci. Comput.*, **35** (2013), B82–B106. https://doi.org/10.1137/110838376
3. S. C. Brenner, Korn's inequalities for piecewise H^1 vector field, *Math. Comput.,* **73** (2004), 1067–1087.
4. F. Brezzi, M. Fortin, *Mixed and hybrid finite element methods*, New York: Springer Verlag, 1991. https://doi.org/10.1007/978-1-4612-3172-1

5. J. Camaño, G. N. Gatica, R. Oyarzúa, R. R. Baier, P. Venegas, New fully-mixed finite element methods for the Stokes-Darcy coupling, *Comput. Method. Appl. M.*, **295** (2015), 362–395. https://doi.org/10.1016/j.cma.2015.07.007
6. Y. Cao, M. Gunzburger, X. He, X. Wang, Parallel, non-iterative, multi-physics domain decomposition methods for time-dependent Stokes-Darcy systems, *Math. Comput.*, **83** (2014), 1617–1644. https://doi.org/10.1090/s0025-5718-2014-02779-8
7. Y. Cao, M. Gunzburger, X. Hu, F. Hua, X. Wang, W. Zhao, Finite element approximation for Stokes-Darcy flow with Beavers-Joseph interface conditions, *SIAM J. Numer. Anal.*, **47** (2010), 4239–4256. https://doi.org/10.1137/080731542
8. A. Cesmelioglu, B. Riviére, Existence of a weak solution for the fully coupled Navier-Stokes/Darcy-transport problem, *J. Differ. Equations*, **252** (2012), 4138–4175. https://doi.org/10.1016/j.jde.2011.12.001
9. W. Chen, M. Gunzburger, F. Hua, X. Wang, A parallel Robin-Robin domain decomposition method for the Stokes-Darcy system, *SIAM J. Numer. Anal.*, **49** (2011), 1064–1084. https://doi.org/10.2307/23074323
10. W. Chen, M. Gunzburger, D. Sun, X. Wang, Efficient and long-time accurate second-order methods for the Stokes-Darcy system, *SIAM J. Numer. Anal.*, **51** (2013), 2563–2584. https://doi.org/10.1137/120897705
11. W. Chen, F. Wang, Y. Wang, Weak Galerkin method for the coupled Darcy-Stokes flow, *IMA J. Numer. Anal.*, **36** (2016), 897–921. https://doi.org/10.1093/imanum/drv012
12. Y. Chen, X. Zhao, Y. Huang, Mortar element method for the time dependent coupling of Stokes and Darcy flows, *J. Sci. Comput.*, **80** (2019), 1310–1329. https://doi.org/10.1007/s10915-019-00977-4
13. P. G. Ciarlet, *The finite element method for elliptic problems*, Society for Industrial and Applied Mathematics, 2002. https://doi.org/10.1137/1.9780898719208
14. M. Crouzeix, P. A. Raviart, Conforming and nonconforming finite element methods for solving the stationary Stokes equation, *RAIRO Anal. Numer.*, **7** (1973), 33–75. https://doi.org/10.1051/m2an/197307R300331
15. M. Discacciati, E. Miglio, A. Quarteroni, Mathematical and numerical models for coupling surface and groundwater flows, *Appl. Numer. Math.*, **43** (2002), 57–74. https://doi.org/10.1016/S0168-9274(02)00125-3
16. J. Douglas, R. E. Ewing, M. F. Wheeler, The approximation of the pressure by a mixed method in the simulation of miscible displacement, *RAIRO Anal. Numer.*, **17** (1983), 17–33. https://doi.org/10.1093/qjmam/36.4.505
17. V. J. Ervin, Approximation of coupled Stokes-Darcy flow in an axisymmetric domain, *Comput. Method. Appl. M.*, **258** (2013), 96–108. https://doi.org/10.1016/J.CMA.2013.02.004
18. V. J. Ervin, E. W. Jenkins, S. Sun, Coupled generalized nonlinear Stokes flow with flow through a porous medium, *SIAM J. Numer. Anal.*, **47** (2009), 929–952. https://doi.org/10.1137/070708354
19. G. N. Gatica, R. Oyarzúa, F. J. Sayas, A residual-based a posteriori error estimator for a fully-mixed formulation of the Stokes-Darcy coupled problem, *Comput. Method. Appl. M.*, **200** (2011), 1877–1891. https://doi.org/10.1016/j.cma.2011.02.009

20. V. Girault, P. A. Raviart, *Finite element methods for Navier-Stokes equations*, Berlin: Springer Verlag, 1986. https://doi.org/10.1007/978-3-642-61623-5
21. V. Girault, D. Vassilev, I. Yotov, Mortar multiscale finite element methods for Stokes-Darcy flows, *Numer. Math.*, **127** (2014), 93–165. https://doi.org/10.1007/s00211-013-0583-z
22. P. Hessari, Pseudospectral least squares method for Stokes-Darcy equations, *SIAM J. Numer. Anal.*, **53** (2015), 1195–1213. https://doi.org/10.1137/140954350
23. T. Karper, K. A. Mardal, R. Winther, Unified finite element discretizations of coupled Darcy-Stokes flow, *Numer. Meth. Part. D. E.*, **25** (2009), 311–326. https://doi.org/10.1002/num.20349
24. W. J. Layton, F. Schieweck, I. Yotov, Coupling fluid flow with porous media flow, *SIAM J. Numer. Anal.,* **40** (2003), 2195–2218. https://doi.org/10.1137/S003614290139276
25. R. Li, J. Li, X. He, Z. Chen, A stabilized finite volume element method for a coupled Stokes-Darcy problem, *Appl. Numer. Math.*, **133** (2018), 2–24. https://doi.org/10.1016/j.apnum.2017.09.013
26. K. Lipnikov, D. Vassilev, I. Yotov, Discontinuous Galerkin and mimetic finite difference methods for coupled Stokes-Darcy flows on polygonal and polyhedral grids, *Numer. Math.*, **126** (2014), 321–360. https://doi.org/10.1007/s00211-013-0563-3
27. A. Márquez, S. Meddahi, F. J. Sayas, A decoupled preconditioning technique for a mixed Stokes-Darcy model, *J. Sci. Comput.*, **57** (2013), 174–192. https://doi.org/10.1007/s10915-013-9700-5
28. A. Márquez, S. Meddahi, F. J. Sayas, Strong coupling of finite element methods for the Stokes-Darcy problem, *IMA J. Numer. Anal.*, **35** (2015), 969–988. https://doi.org/10.1093/imanum/dru023
29. G. Pacquaut, J. Bruchon, N. Moulin, S. Drapier, Combining a level-set method and a mixed stabilized P1/P1 formulation for coupling Stokes-Darcy flows, *Int. J. Numer. Meth. Fl.*, **69** (2012), 459–480. https://doi.org/10.1002/fld.2569
30. B. Riviére, Analysis of a discontinuous finite element method for the coupled Stokes and Darcy problems, *J. Sci. Comput.*, **22** (2005), 479–500. https://doi.org/10.1007/s10915-004-4147-3
31. B. Riviére, I. Yotov, Locally conservative coupling of Stokes and Darcy flows, *SIAM J. Numer. Anal.*, **42** (2005), 1959–1977. https://doi.org/10.1137/S0036142903427640
32. H. Rui, R. Zhang, A unified stabilized mixed finite element method for coupling Stokes and Darcy flows, *Comput. Method. Appl. M.*, **198** (2009), 2692–2699. https://doi.org/10.1016/j.cma.2009.03.011
33. H. Rui, J. Zhang, A stabilized mixed finite element method for coupled Stokes and Darcy flows with transport, *Comput. Method. Appl. M.*, **315** (2017), 169–189. https://doi.org/10.1016/j.cma.2016.10.034
34. I. Rybak, J. Magiera, A multiple-time-step technique for coupled free flow and porous medium system, *J. Comput. Phys.*, **272** (2014), 327–342. https://doi.org/10.1016/j.jcp.2014.04.036
35. L. Shan, H. Zheng, W. J. Layton, A decoupling method with different subdomain time steps for the nonstationary Stokes-Darcy model, *Numer. Meth. Part. D. E.*, **29** (2013), 549–583. https://doi.org/10.1002/num.21720
36. M. C. Shiue, K. C. Ong, M. C. Lai, Convergence of the MAC Scheme for the Stokes/Darcy Coupling Problem, *J. Sci. Comput.*, **76** (2018), 1216–1251. https://doi.org/10.1007/s10915-018-0660-7

37. D. Vassilev, C. Wang, I. Yotov, Domain decomposition for coupled Stokes and Darcy flows, *Comput. Method. Appl. M.*, **268** (2014), 264–283. https://doi.org/10.1016/j.cma.2013.09.009

38. D. Vassilev, I. Yotov, Coupling Stokes-Darcy flow with transport, *SIAM J. Sci. Comput.*, **31** (2009), 3661–3684. https://doi.org/10.1137/080732146

39. W. Wang, C. Xu, Spectral methods based on new formulations for coupled Stokes and Darcy equations, *J. Comput. Phys.*, **257** (2014), 126–142. https://doi.org/10.1016/j.jcp.2013.09.036

40. M. F. Wheeler, A priori L^2 error estimate for Galerkin approximation to parobolic partial differential equations, *SIAM J. Numer. Anal.*, **10** (1973), 723–759. https://doi.org/10.1137/0710062

41. J. Zhang, H. Rui, A stabilized Crouzeix-Raviart element method for coupling Stokes and Darcy-Forchheimer flows, *Numer. Meth. Part. D. E.*, **33** (2017), 1070–1094. https://doi.org/10.1002/num.22129

42. L. Zhao, E. T. Chung, E. J. Park, G. Zhou, Staggered DG method for coupling of the Stokes and Darcy-Forchheimer problems, *SIAM J. Numer. Anal.*, **59** (2021), 1–31. https://doi.org/10.1137/19M1268525